Chapter 6

Ferrosilicon and Silicon Technology

Merete Tangstad
Norwegian University of Science and Technology, Trondheim, Norway

Chapter Outline

6.1 INTRODUCTION TO SILICON AND ITS FERROALLOYS

In the liquid state, silicon has metallic properties regarding thermal and electrical conductivity, but in the solid state, it is a semiconductor and is called a metalloid. Due to its visual similarities in color and reflectance, it is often, misleadingly, referred to as a metal. Also when it comes to the production process, silicon may be produced in equipment used for metals production, such as manganese alloys and chromium alloys, and thus it is grouped with these alloys.

Before the 19th century, all elements discovered were produced by reduction with either hydrogen or carbon, but the later discovery of electrolysis has

Handbook of Ferroalloys. http://dx.doi.org/10.1016/B978-0-08-097753-9.00006-X

allowed the extraction of potassium, sodium, calcium, barium, strontium, cadmium, and aluminum. In 1824, silicon was produced by the Swedish chemist Jöns Jacob Berzelius, and he named the new material "silicium." As this material was closer in properties to bor*on* and carb*on* than materials like magnesi*um* and calci*um,* the Scottish chemist Thomas Thomson renamed it "silic*on*" some years later. In the literature, both names are still in common use in some countries.

The development of the industrial process of silicon production took almost a century (Schei et al., 1998; Vishu et al., 2005). With the development of the electric arc furnace by Paul Héroult, the first commercial plant was started in the United States in 1907, where high silicon ferrosilicon and silicon could be produced industrially. Frank Tone of Carborundum Co. was the first to commercialize the production of silicon. In the 1920s, silicon use in aluminum alloying increased steadily. In the 1930s, silicon application in chemicals and silicones increased, and the next boost for silicon came after the 1950s for photovoltaic applications, followed by the modern-day silicon demand in electronics. To be used as a semiconductor, silicon needs to be pure, and hence the metallurgical grade Si (MG-Si) must be further refined to fulfill requirements. Whereas MG-Si usually has 98.5% to 99.5% Si, the impurity content in photovoltaic devices, such as solar cells, must be in the ppm level and in electronic devices the impurity content must be in the ppb level. The most used refining method for both products is the Siemens process, where the Si is transformed to silicon–chlorine gases, which are distilled and then reduced to silicon.

The development of ferrosilicon technology corresponded with progress in the steel industry. In the 19th century, low silicon ferroalloys (~20% Si), known as silvery pig iron, were produced in blast furnaces, but since the 1920s all production has been moved to submerged arc electric furnaces, as they alone offer the only possibility of high silicon ferroalloys smelting.

6.1.1 Properties of Silicon

Silicon is the second, after oxygen, most abundant element in Earth's lithosphere, occurring naturally in the form of silica (silicon oxide) and silicates and constituting over 25% of the crust. Silicon belongs to group IV of the periodic table with an atomic weight of 28.08 and an external electron shell configuration of $3s^2 3p^2$. As an analog of carbon, silicon might have oxidation states between 1 and 4, the latter being the most stable. Silicon lattice has a cubic, face-centered (FCC), diamond-type structure with lattice period 0.54307 nm at ambient conditions, giving silicon a density of 2.33 g/cm^3. The melting point of silicon is 1414°C, and the boiling point is 3250°C. The density of liquid silicon is temperature dependent (Schei et al., 1998): $\rho_{\text{liq}} = 2553 - 0.45(T - T_m)$ in kg/m^3, with T_m being the melting temperature. Liquid silicon solubilizes most elements to a low degree, and hence the density will not greatly depend on dissolved elements. However, if

iron is present, it will dramatically affect the density. At 1450°C the density of the Fe-Si alloys might be given as $\rho(\mathrm{FeSi})_{\mathrm{liq}} = 7106 \cdot \exp(-0.0107 \cdot \%\ \mathrm{Si})$ in kg/m^3, where silicon content is expressed in wt. %.

6.1.2 Silicon Interaction with Other Elements

The interaction of silicon with oxygen and their compounds (silicon oxides) forms the basis not only for most metallurgical processes, but also for almost all known Earth minerals based on silicates. Silicon forms two oxides: silica (SiO_2) and silicon monoxide (SiO). Silica may exist in several phase modifications (quartz, cristobalite, tridymite, etc.), the transformations for which are shown in Section 6.2.1. At ambient conditions, ß-quartz modification is the most stable. Silicon monoxide is metastable in its condensed state and easily decomposes to silicon and SiO_2, but it is stable in a gas phase at higher temperatures. A detailed analysis of the phase equilibria and thermodynamics relating to the Si-O system was made by Schnurre et al. (2004). They considered the stable condensed phases in this system at normal pressure as quartz, cristobalite, and liquid, besides solid and liquid silicon. The Si-O phase diagram and the enlarged silicon-rich region are shown in Figure 6.1.

The solubility of oxygen in solid and liquid silicon has been studied extensively as it is important for high-quality silicon production. Data analyzed (Schnurre et al., 2004; Tang et al., 2010) show that the three-phase equilibrium L = (Si) + cristobalite is a eutectic reaction, where the eutectic composition was calculated as 47.3 ppm O (at.) in solid solution and 54.2 ppm O (at.) in the liquid phase, but the eutectic temperature is only 0.003 K below the melting point of silicon. As Schnurre et al. (2004) pointed out, this extremely small melting point depression is certainly beyond any experimental determination and a direct consequence of the variation of assessed oxygen solubility in solid and liquid silicon (Tang et al., 2010). Thus, in many published phase diagrams, liquidus and solidus lines are practically indistinguishable near the pure silicon composition.

With carbon silicon forms one stable silicon carbide molecule (SiC). The phase equilibrium diagram Si-C is shown in Figure 6.2.

Silicon carbide does not melt but decomposes peritectically at ~2545°C. Gas phase over SiC has a complex composition, which depends on temperature (at 2000 K gas phase contains % (vol): 86.5 Si, 6.1 SiC_2, and 7.4 SiC). The density of silicon carbide is 3.22 g/cm^3 and besides two phase modifications α-SiC (hexagonal, $a = 0.3078$ nm, $c = 0.2518$ nm) and ß-SiC (cubic, $a = 0.43596$ nm), the α-SiC might exist in different polytypes (Fig. 6.3). The number of known polytypes is about 240, and they are formed by different arrangements and stacking of the layers into a single structure.

The most typical categories are 6H, 15R, and 4P (the digit tells the number of stacked layers, and the letter identifies the type of stack, hexagonal [H] or rhombohedral [R]), although some other forms also have practical value—for

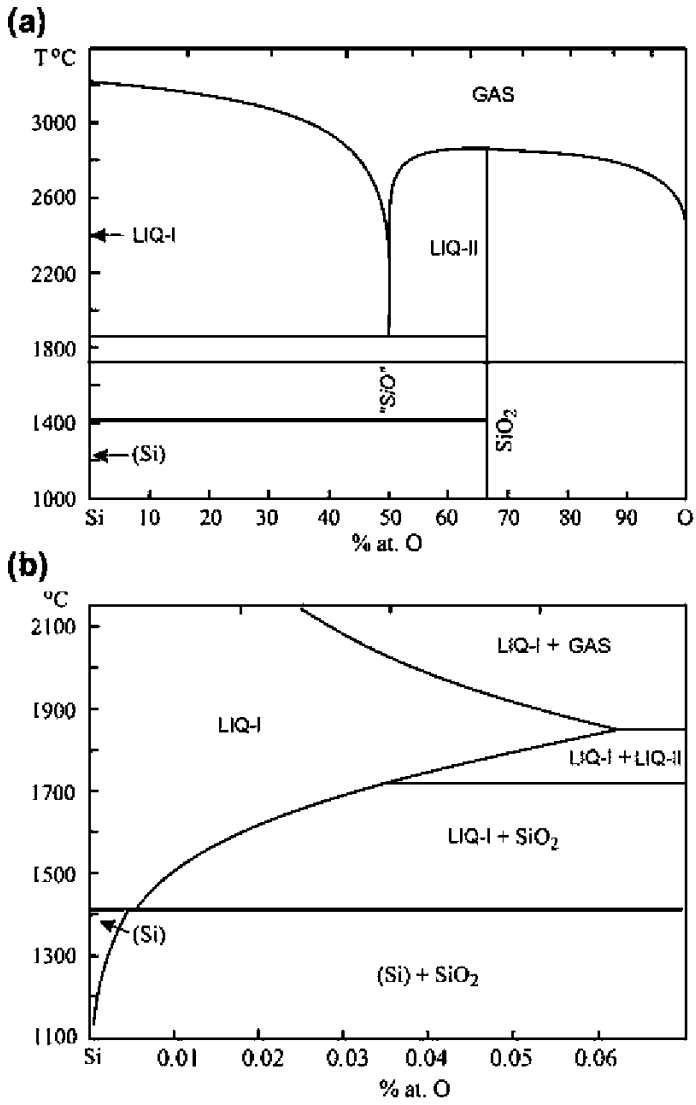

FIGURE 6.1 The equilibrium Si-O phase diagram (a) and its enlargement for the Si-rich domain (b).

example, polytype 9T crystallizes from very pure silicon melts (Inoue et al., 1971). In the SiC lattice, every carbon atom is placed into the tetrahedron of four Si atoms, and every Si atom, respectively, into C-tetrahedron. Tetrahedra [SiC_4] and [CSi_4] might be stacked in parallel or antiparallel, forming similarly oriented 2-4 hyperlayers (Gasik and Gasik, 2011). The ß-phase transforms into α-SiC at temperatures over 2100°C. The density of α-SiC is temperature

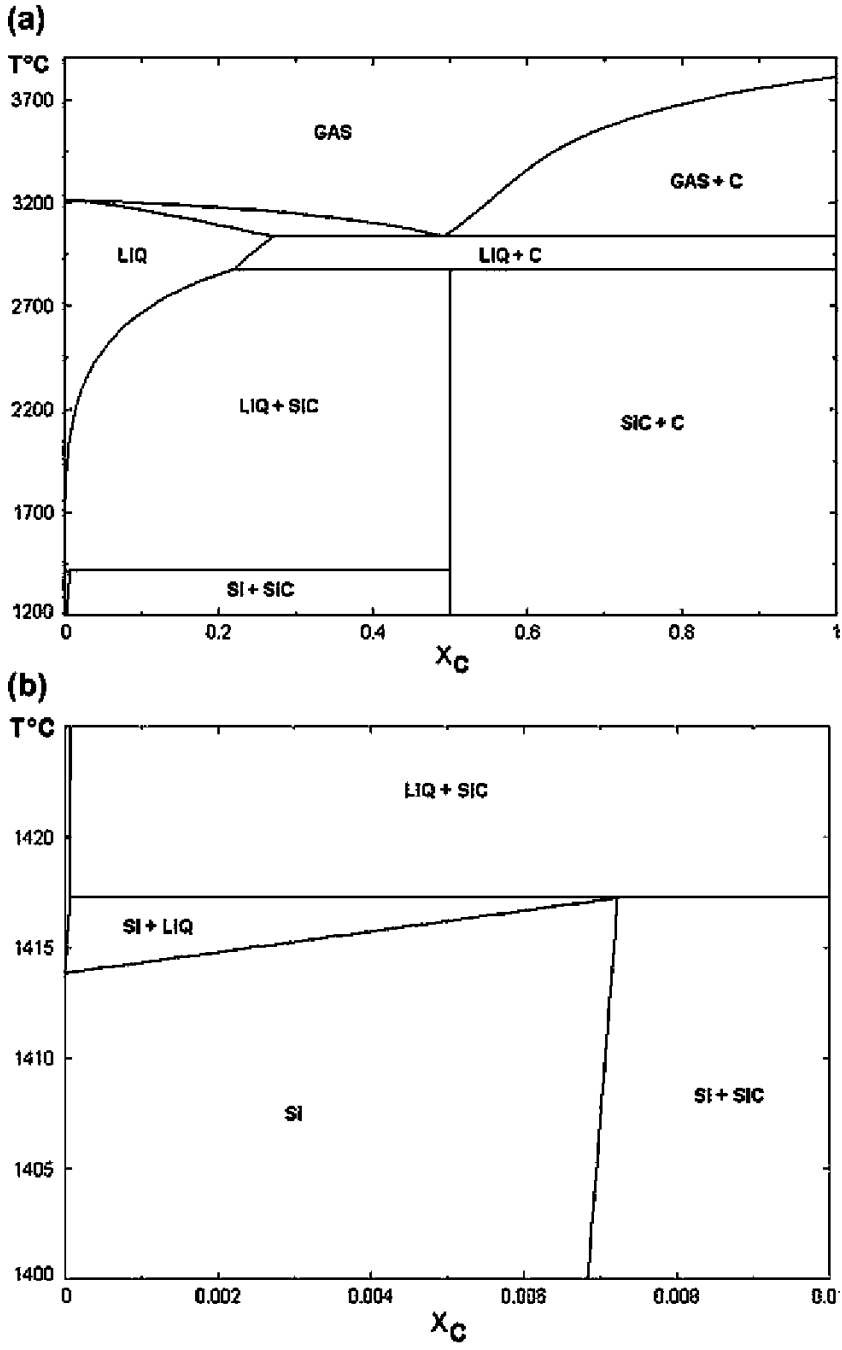

FIGURE 6.2 The equilibrium Si-C phase diagram (a) and its enlarged part in the Si-rich domain (b).

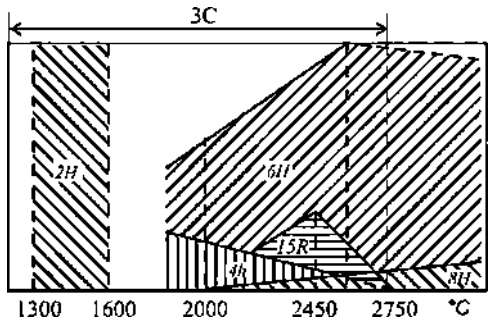

FIGURE 6.3 Approximate share of coexisting SiC polytypes. *(From Gasik and Gasik, 2011.)*

dependent and could be given for α-SiC as $\rho_{\alpha\text{-SiC}} = 3211–0.056 \cdot T(^{\circ}C)$, in kg/m^3. Pure silicon carbide is colorless, but the presence of impurities gives green or gray color tints. In the furnace, produced silicon will be saturated with carbon and oxygen, as both SiC and SiO_2 are present in much excess in the high temperature zone. As the melt temperature is decreased during tapping and solidification, the solubility will decrease so SiO_2 and SiC precipitate. The solubility of oxygen is higher in the presence of iron (in ferrosilicon), but the solubility of carbon is lower compared to that for pure silicon.

Like oxygen and carbon, sulfur has very low solubility in silicon ($< \sim 10^{-8}$ %), but it forms volatile sulfides SiS and SiS_2. Sulfur also reacts with SiC over 900°C with the formation of SiS_2 and CS_2. These interactions are important for understanding the behavior of sulfur in the furnace, as sulfur is brought into the process with coke and other charge materials.

There are also a number of other impurity elements that will follow with the raw materials into the furnace and dissolve in silicon. The solubility is especially important when it comes to the solidification process, either during casting or in the refining step. The solubility of some elements is shown in Figure 6.4, which shows that among others, B, As, and P have relatively high solubility and their concentration will hence not be reduced dramatically during a directional solidification step. Tang et al. (2010) did an assessment of solubility, the activity coefficient, and the diffusivity of various elements in silicon.

The equilibria in the Si-O-C system are the most critical for understanding the development of the silicon oxide reduction process in the smelting of silicon and ferrosilicon. In this system, equilibrium solid phases are SiO_2 (solid or liquid), Si (solid or liquid), SiC (solid), carbon, and the gas phase (CO, CO_2, SiO, SiO_2, O_2, SiC, SiC_2, Si_2, Si_3, C_2, C_3, Si_2C, Si_2C_2, Si_3C, etc.). As the industrial furnace is highly reducing, the main gas species will be CO and SiO. The main reactions in the Si-O-C system might be presented as equilibrium SiO pressure versus temperature (Fig. 6.5). Note that this figure does not show the true predominance phase diagram, but an expression of different equilibrium reactions, which defines zones of eventual coexistence of different phases.

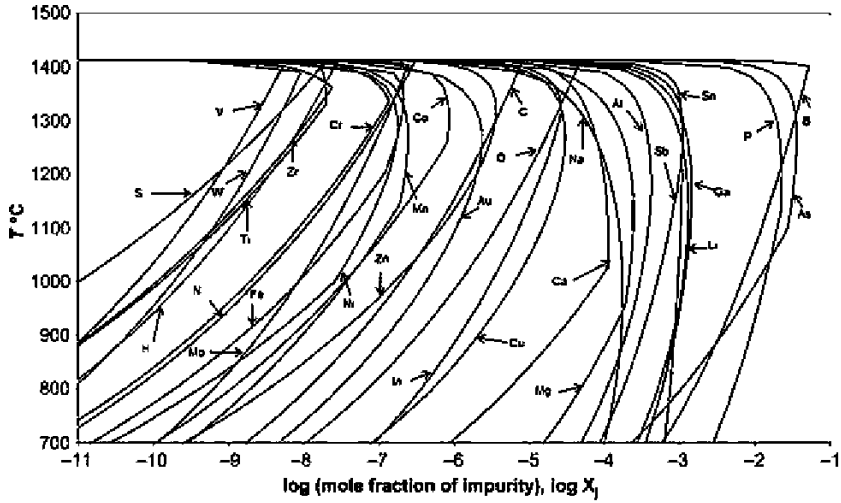

FIGURE 6.4 Solubility of different impurities in silicon. *(From Tang et al., 2010.)*

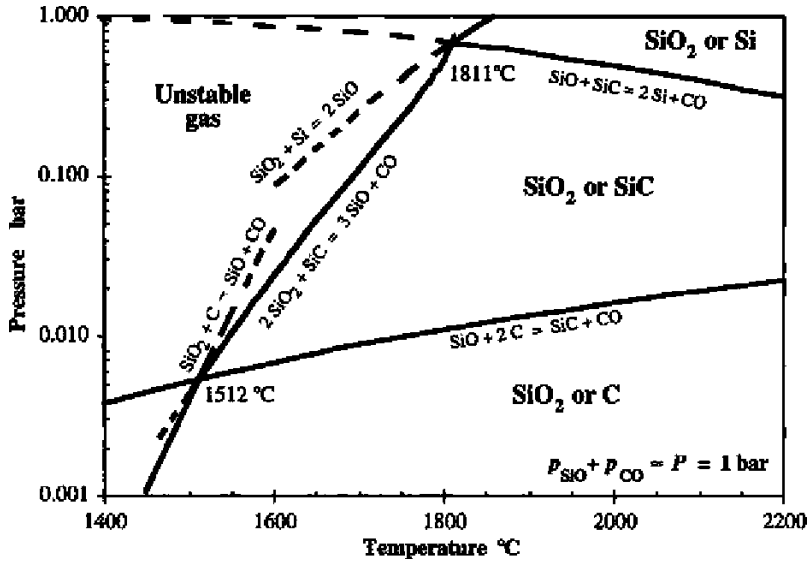

FIGURE 6.5 Partial SiO pressure versus temperature for equilibrium with different condensed phases at a total gas pressure of 1 atm. *(From Schei et al., 1998.)*

With this diagram, the conditions for silicon reduction might be understood at reasonably high temperatures (>1800°C) and high SiO partial pressures. A higher SiO pressure and a higher temperature will increase the driving force to produce silicon. Carbon is only present at low temperatures and low SiO

pressures—when SiO pressure increases, carbon will react to form SiC. Hence, in a furnace where temperatures are well above 1000°C, SiC will be the stable carbon-containing phase in the system.

With Gibbs energy minimization, the phase predominance diagrams have been constructed for this system at prescribed temperature and total pressure (Gasik and Gasik, 2010). All solid phases were taken as pure substances, but gas was considered as real, not ideal. An additional feature is computing on the isobar of P = 1 bar, which is shown in Figure 6.6 as a line of plus signs (+++).

The interaction of silicon with iron is the basis for the formation of FeSi alloys in a wide range of compositions. Silicon is a ferrite-stabilizing element and narrows the γ-Fe stability area (Fig. 6.7).

The maximum solubility of silicon in γ-Fe is 1.63% wt. Si. The two-phase region (α + γ) extends to 1.94% Si. A number of silicides are formed in the Fe-Si system: Fe_3Si, Fe_2Si, Fe_5Si_3, FeSi, and $FeSi_2$. The latter exists in two modifications: high-temperature $FeSi_2$ (HT) at 937° to 1220°C and low-temperature $FeSi_2$ (LT), which is below 937°C. The high-temperature phase is a nonstoichiometric compound, which exists in a certain range of concentrations of silicon, usually described as $FeSi_{2.3}$. However, it has been shown that the correct structural formula of this silicide is Fe_xSi_2, which transforms to an LT-phase below 937°C according to the reaction (Zubov and Gasik, 2002):

$$y\ \mathrm{Fe_xSi_2} \rightarrow \frac{x}{y}\mathrm{FeSi_2} + 2\left(y - \frac{x}{y}\right)\mathrm{Si}.$$

Silicide Fe_3Si has a wide composition range, two modifications, and an ordering-disordering transformation (Fig. 6.8). A strong interaction between iron and silicon in the solid state is reflected also in the liquid. At 1600°C, the thermodynamic stability of clusters (associates) in the Fe-Si melt was determined to correspond to the following ratios: [FeSi]:[Fe_3Si]:[$FeSi_2$]:[Fe_5Si_3] = as 17.2:6.6:1.9:1, respectively, indicating that equimolar concentration FeSi is the most favorable.

6.2 RAW MATERIALS, SILICON, AND FERROSILICON COMPOSITIONS

6.2.1 Sources of Silica

Silicon and its ferroalloys are produced by reducing silica-rich raw materials (quartzite or quartz) with carbon. Relatively pure silica (SiO_2), more frequently known as the mineral quartz, is usually found in pegmatite or hydrothermal bodies. The ore body containing the mineral quartz and smaller amounts of gangue is currently referred to as quartzite. Quartzite is typically formed metamorphic to quartz-rich sandstone. Hence, the terms *quartz* and *quartzite* are both used to describe the raw material for silicon production. From the

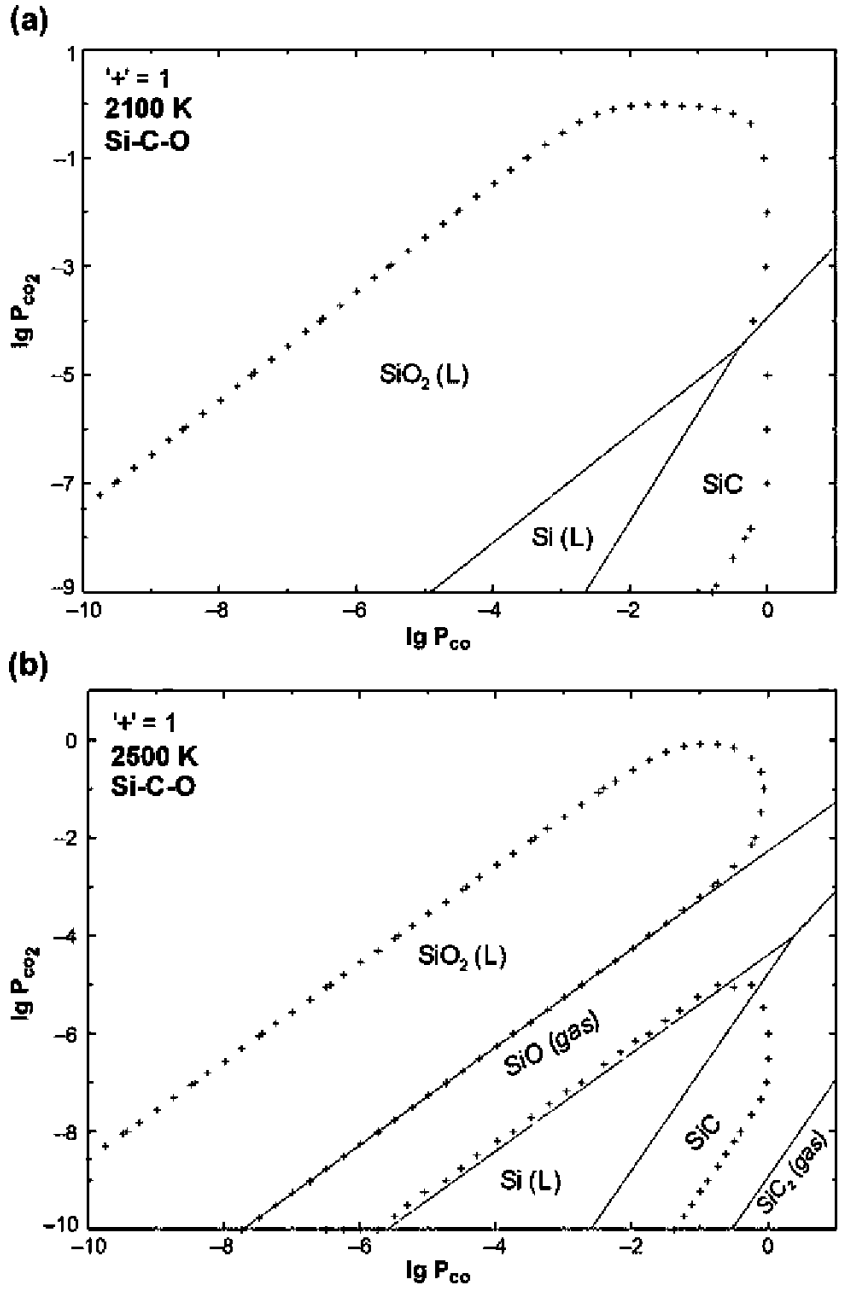

FIGURE 6.6 The phase predominance diagrams in the Si-O-C system for 2100 K (a) and 2500 K (b).

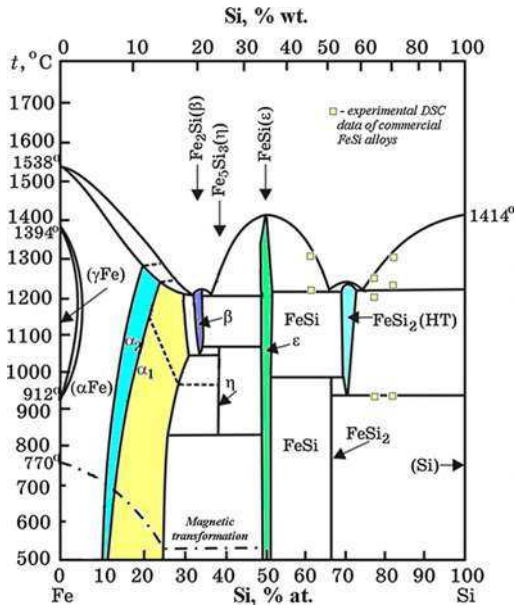

FIGURE 6.7 Equilibrium Fe-Si diagram. Experimental data (by M. M. Gasik) are shown for commercial FeSi alloys with 45%, 65%, and 70% Si.

FIGURE 6.8 Example of thermal expansion of quartz specimen during heating between 1750° and 1800°C.

metallurgical considerations, quartzite is used for more impure materials, whereas quartz is used for the purer ore bodies.

The most stable phase of silicon oxides is quartz (SiO_2), having a melting point of 1726°C and a boiling point of 2275°C. Silicon oxide SiO_2 also has several modifications that are more stable in a certain temperature range (Zubov and Gasik, 2002). The sequence of the quartz transformations might be presented as in Table 6.1. Transformations of quartz on heating and cooling are accompanied by a change in volume that sometimes leads to a premature cracking of quartz grains (quartzite) at the top of the furnace.

TABLE 6.1 Schematic of Basic Quartz Phase Transformations

α-quartz	α-tridymite	α-cristobalite	
(870°C) →	(1470°C) →	(1720°C) →	Melt
↕ 574°C	↕ 163°C	↕ 180-275°C	↕
ß-quartz	ß-tridymite	ß-cristobalite	Glass (quenched)
	↕ 117°C		
	γ-tridymite		

It is worth noting that silica phases might have other structural forms but they have less metallurgical relevance. Transformations shown in Table 6.1 by vertical arrows are usually fast and the volume changes during these transformations are normally <1%. Transformations shown by horizontal arrows are slow and the change of volume between different phases is significant (e.g., α-quartz → α-tridymite adds 14% to 15% to the volume). Aasly (2006) found that after 10 minutes at 1550°C different quartz types would have between 0% and 10% of cristobalite. After 5 h holding at this temperature, the difference between various quartz types was gone, and they all had about 80% of cristobalite fraction.

As ß forms of silica normally have higher stability, most quartz minerals appear in ß form, vein quartz, quartz sand, sandstone, quartzite, flint, and so on. The basic structural unit of the crystal quartz is a silicon–oxygen tetrahedron $[SiO_4]^{4-}$. The distance Si-O is equal to 0.162 nm, and the nearest oxygen atoms are separated by 0.264 nm, resulting in an angle O-Si-O of 109.028°. Tetrahedrons can form a variety of more complex structural configurations, as described in Chapter 3 in more detail.

Many silica-contained minerals might be used for silicon-rich ferroalloys production. However, for ferrosilicon, quartzite is the most common and, for silicon smelting, quartz is the only feasible option, taking into account properties, availability, and purity. For the product and process requirements, the following properties are considered most important (Schei et al., 1998): chemistry (e.g., Al, Ti, P, Fe, and Ca content), lump size (10 to 150 mm preferable), mechanical and thermal strength (sometimes considered in combination), and softening behavior. Some elements from quartz will end up in the silicon metal, and thus the chemical composition of the oxide is perhaps one of the most important characteristics. These elements are typically more noble that Si, and among them the presence of iron, titanium, and boron is not desirable in silicon. Iron, of course, is not the concern in FeSi alloys. The quartzes used for silicon production typically contain more than 99% SiO_2, with major impurities being Al (<0.5), Fe (<0.3), alkali (<0.25), and Ti (<0.02) species.

The lump size distribution is the most important parameter affecting the operation of the furnace. The mechanical strength of quartz is important during

transportation and handling, as well as the thermal strength during heating inside the furnace. Aasly (2006) reported that the fines generation and the strength of the material are dependent on the following major causes: type of quartz, mining procedures, and handling operations during transportation. It was found that even when the drilling and blasting conditions were similar during quartz mining, the resulting quartz product might give different levels of mechanical strength and stability.

Various mechanical loads are applied to quartz during transportation, and the most damaging one is the mechanical stress during drops (total drop height sometimes is ~70 m from the vessel to the furnace). The friability index is used to measure of the mechanical strength of the unheated quartz and is meant to assess how much of the quartz is disintegrating during transport (Aasly, 2006). A Hannover drum is used for tumbling the samples for given time and rate. After tumbling, the material is sieved, and a quantitative measure is found—for example, the percentage that still has the size of the original material and the dust (fines) formation as −2 mm fraction.

The strength of the quartz raw material on heating is linked with the raw quartz properties: with a high content of microcracks from mining and transport, such quartz might disintegrate more easily during heating. The material will more or less disintegrate at elevated temperatures for different reasons (Aasly, 2006). Below the α- to β-quartz transformation (573°C), a decrepitation will occur due to fluid inclusions and the opening of microcracks. At temperatures 900° to 1000°C, decrepitating occurs again due to mica inclusions in the quartz, and over 1300°C all quartz types fracture. The formation of fines was found to increase with the cristobalite formation in quartz.

Although the chemical composition, size distribution, and the mechanical strength are the most used characterization methods for quartz feasibility for smelting in the furnace, other parameters may also be important, such as softening and melting temperature and the volume expansion of quartz.

The softening and melting of various quartz samples may affect the furnace operation. If the quartz used is melting too high in the furnace (i.e., its melting temperature is too low), it will form a sticky mass with the rest of the charge materials. This will prevent gas flow through the charge and hence gas channels will form, leading to a high SiO percentage loss and low Si output. Formation of the liquid slag phase up in the furnace might redirect some electric current paths, taking power off the arc and disturbing arc formation and overall thermal balance of the furnace. Of different investigated industrial quartz samples, heated in CO and nitrogen gas, none of them showed softening tendencies before 1800°C. However, some of them showed high volume expansion, which is believed to correlate to the transformation from quartz to cristobalite as shown in Figure 6.8. It can also be noted that the volume expansion in some of the material is much higher than the

before-mentioned 15% increase, which thus might also be due to other causes.

Quartzites are a group of minerals that consists of quartz and other silica-rich minerals (opal, chalcedon, quartz) accompanied by different clay materials. Quartzites also have 4% to 9% of bounded water. Clays are usually particles <10 μm, composed of silica (30% to 70%), alumina (10% to 40%), and water with impurities of Fe_2O_3, TiO_2, CaO, MgO, K_2O, and Na_2O. Clays are the major source of alumina in quartzites, so they cannot be used directly in silicon and high-Si ferrosilicon smelting. The most typical clay minerals are kaolinite $Al_2O_3 \cdot 2SiO_2 \cdot 2H_2O$, dickite $Al_4[(OH)_8Si_4O_{10}]$, nacrite $Al_4[(OH)_8Si_4O_{10}]$, hydromuscovite $K_x(H_2O)_x[Al_2(AlSi_3O_{10})\ (OH)_{2\text{-}x} \cdot (H_2O)_x]$, and illite $(MgFe)_2(Si,Al_4)O_{10} \cdot [(OH)_2, H_2O]$. The last two are major sources of alkalis in ferrosilicon production. Some typical compositions of quartzites reported from Commonwealth of Independent States (CIS) countries are summarized in Table 6.2 (Gasik and Gasik, 2011).

6.2.2 Carbon Reductants

The choice of carbon reduction material is based on the following three main factors: process, product, and environmental considerations. The material must have the properties needed to achieve a high Si yield in the furnace and it must meet the product specifications. This means that the conditions for impurity elements in the raw materials (as, e.g., phosphorus) must be met. The reduction material will naturally cause the emissions of CO_2. This is inevitable with today's technology. Some elements in the reduction materials will be reduced or evaporated in the process and follow the off-gases. Mercury is one element that will end up in the off-gases and should be avoided in the raw materials.

Besides general requirements for carbon reductants for ferroalloys (Chapter 3), in silicon and ferrosilicon smelting the additional most important requirements are size and SiO reactivity. The size of the particles will affect the permeability of the charge burden as well as the SiO reactivity. If the carbon particles are too fine, a high SiO reactivity will be obtained, but at the same time the gas permeability will decrease. Also smaller particles (<1.5 mm) may be taken by the gas flow, thus decreasing the process availability of the carbon added. The size of the carbon material is typically between 1 to 30 mm, according to Schei et al. (1998).

Myrvågnes (2008) investigated SiO reactivity, and the following summary is based on his work. His review showed that there are a number of recipes for carbon mixes that are used worldwide in Si smelting furnaces (Fig. 6.9). Based on a costs and availability, the reduction material can be based on fuels like coal or charcoal. Some producers also use petroleum coke. Metallurgical coke is not much used, as it gives lower SiO reactivity.

All producers use woodchips to increase the permeability of the burden. As shown later, the large number of condensates in the silicon furnace may easily

TABLE 6.2 Some Typical Compositions of Quartzite Minerals

	Composition, % wt.						
Origin	**SiO_2**	**Fe_2O_3**	**Al_2O_3**	**CaO**	**MgO**	**TiO_2**	**P_2O_5**
Russia/Ural-1	98–99	0.3–0.4	0.25–0.45	—	—	—	—
Russia/Ural-2	98–98.5	0.41	0.24	0.7	—	0.14	—
Russia/Ural-3	97–98	0.2–0.4	0.9–1.3	0.2–0.4	0.1–0.3	—	—
Russia/Center	96–98	0.7–0.9	0.8–1.2	0.3–0.6	0.04–0.2	0.07	—
Russia/South	96–98	0.4–0.9	0.2–1	0.3–0.7	0.1–0.3	—	—
Russia/Siberia	98.4	0.4	0.5	0.52	0.35	—	—
Georgia	96–96.5	1–2.6	0.2–0.5	0.7	0.2–0.5	—	—
Ukraine/East	97.5–98.5	<2	<1.7	0.8	–	—	—
Urkaine/Center	97–98	0.5–1	0.4–1.2	0.2–1.	0.2–0.4	—	—
Ukraine/West	98–98.6	0.1–0.2	0.4–0.7	—	—	—	—
Kazakhstan/East	95–99	0.2–2.8	0.4–1.9	0.1–0.2	0.03–0.2	0.02–0.06	0.01–0.02
Uzbekistan	95–96.5	0.2–1.4	0.8–1	0.2–1.3	<0.15	—	—

FIGURE 6.9 Comparison of various recipes of carbon reductants for silicon production by different sources. *(From Myrvågnes, 2008.)*

clog the voids in the burden. Hence, compared to other metallurgical furnaces, extreme measures, like using woodchips, must be taken to ensure good permeability. The typical raw materials used in silicon production are thus coal, charcoal, petroleum coke, and char for reduction purposes and woodchips for permeability (Myrvågnes, 2008).

Coal is a fossil carbonaceous material that is fairly commonly used as a reductant in the silicon process. Properties of coal are determined by organic materials from which it is the solid product, conditions at the time of deposition, and parameters that influence the maturity (see Chapter 3). The main properties of coal affecting both the process and the purity of the produced metal are rank, maceral composition, and amount and origin of mineral inclusions in the coal.

Metallurgical coke is the solid residue after a controlled carbonization of bituminous coal. As most of the metallurgical coke is used in the blast furnace production of pig iron, the main requirements are high strength and low reactivity toward CO_2. As properties of metallurgical coke do not correlate well with the requirements for reduction materials in the silicon process, char and reactive coke are used more commonly than metallurgical coke.

Char constitutes carbonization products from wood, activated carbons, or coal that do not pass through a plastic stage during pyrolysis and carbonization. Chars can be differentiated from metallurgical cokes by the level of anisotropy, with the former being isotropic and the latter characterized by a high degree of anisotropy.

Charcoal is a reduction material of biological origin and has been produced for centuries if not millennia. Charcoal for the silicon smelting process is produced by pyrolysis and carbonization of wood at moderate heating rates. The process can be divided into the following main stages: heating and drying ($<$110°C), wood endothermic (110° to 270°C) and exothermic (270° to 400°C)

decomposition, charcoal formation with some residual tar (~400°C), completion of carbonization (~500°C), and finally gasification and the degradation of charcoal (500° to 1000°C).

Petroleum coke (petrocoke) is a by-product of the oil refining process, generated in delayed coking. The heavy fractions from crude oil distillation are heated to ~500°C with partial cracking, generating lighter hydrocarbons and a solid residue, which is petroleum coke. The petroleum coke is usually divided into sponge-, shot- and needle-like coke.

Including woodchips in the raw materials recipe results in a higher permeability in the furnace, thus contributing to a better distribution of the gas flow through the burden and minimizing the effects of blowing.

In the silicon smelting process, one important property of the reduction material is its ability to react with SiO gas to increase the silicon yield in the furnace: $2C + SiO(g) = SiC + CO(g)$. Several models of mechanism of this reaction have been investigated, and it was found that the rate-determining step would be a mixture of gas diffusion in and out to the reaction zone and the chemical reaction itself. Myrhaug (2003) compared different theoretical models and found that some particles like charcoal could be described by the shrinking core model, whereas metallurgical coke did not follow the same typical topochemical model. When describing a packed bed, the shrinking core model gave the best result.

In addition to the single particle reactivity, tests of industrial materials usually show more correct results as several particles can be investigated simultaneously. One method commonly used to test for industrial carbon materials used in the silicon industry is the SINTEF reactivity test. In this test, the off-gas composition is measured and correlated with materials reactivity. The reactor contains three distinct parts: first a SiO generator, then a reaction chamber, and, on top, a condensing chamber. These reactors are placed in a vacuum graphite tube resistance furnace. In the SiO generator, the pellets made of fine ground α-quartz (SiO_2) and SiC powder are loaded and heated in Ar gas to a fixed temperature where they produce gas with 4.5% CO and 13.5% SiO according to the reaction $2SiO_2 + SiC = 3SiO(g) + CO(g)$. This gas enters the reaction chamber where the tested reduction material is placed in a bed. The SiO in the gas will react with carbon material to produce more CO: $SiO(g) + C = SiC + CO(g)$, and the SiO concentration in the reacted gas phase should decrease.

If a highly reactive material is used and all SiO gas is consumed, the off-gas from the carbon bed will contain very low amounts of SiO gas. When all tested carbon material is consumed and transformed into SiC, the off-gas will again contain 13.5% SiO, as SiO has no reaction anymore with SiC. The transition period from low SiO content to high SiO content in the off-gas is thus fast for high reactivity materials. If a low reactive carbon material is used, the transition from low SiO content to high SiO content is slower. Hence, a measure of reactivity might be the amount of unreduced SiO gas present

until the CO content reaches 10%. After the gas leaves the reaction chamber, it cools in the condensation chamber where the SiO decomposes into SiO_2 and Si in alumina tubes. The reactivity of different carbon reductants measured by this method could be roughly ranked as "charcoal > coals > cokes," although various groups of raw materials have similarly closer reactivities. Myrvågnes (2008) determined that the most important parameters affecting the SiO reactivity were the rank of the coal, the ratio of fusible macerals versus infusible macerals, the density, and the amount and composition of mineral matter (ash).

6.2.3 Compositions of Silicon and Ferrosilicon

Silicon and ferrosilicon can be used in a number of applications and can be divided into four main product groups.

First, in steelmaking, silicon application has many features. As an alloying element, it provides solid solution strengthening in HLSA and some other steels, improves high-temperature oxidation resistance (Cr-Mo-V and stainless steels with 1% to 2% Si), and ensures lower electric losses in electric steels (e.g., "soft magnetic" steels in transformers, electric motors, and generators). Deoxidation and alloying of steel and cast iron is the largest application of ferrosilicon. Ferrosilicon reduces the oxidation of valuable elements like Cr in stainless steel production. It is also used as an alloying element to increase the elasticity, tensile yield, and annealing resistance in steels. In cast iron it is used, together with other elements, as an inoculant to induce graphite nucleation. Although the main type of silicon addition in steelmaking is in the form of ferrosilicon (FeSi) and ferrosilicon–manganese (FeSiMn), some other silicon ferroalloys are also frequently used (Vishu et al., 2005; Young, 2001).

Second, a large part of the produced silicon is used as an alloying element in aluminum to enhance the mechanical properties of cast and wrought aluminum alloys. As iron is a detrimental element in aluminum, the iron content of the silicon for these purposes must be controlled.

The third important area is the utilization of silicon in the chemical industry to produce silicones and similar derivatives. Silicones can be liquid oil, grease, rubber, and solid resin and are chemically inert, water repellent, and stable up to 400°C. They are used for medical applications, electric insulators, protective coatings, hydraulic fluids, and lubricants. The most important property of the silicon to this group of customers is the content of impurity elements, but the structure and grain/lump size of silicon are also important. Besides pure silicon, some high silicon ferrosilicon may be used.

Finally, as a semiconductor, silicon is widely used as a raw material in the electronics industry. For these applications, purity and dopants control are critical factors, and hence the metallurgical grade Si (MG-Si) must be further refined to fulfill its requirements. Although MG-Si usually has silicon content

from 98.5% to 99.5% Si, the impurity content in, for example, solar photovoltaic devices must be in the ppm level and for electronic devices it must be in the ppb level. The most used refining method for both products is the Siemens process where the raw material silicon is transformed to silicon–chlorine gases, which are distilled and then reduced back to pure silicon.

Since the beginning of the 21st century, the production of silicon has increased gradually from 1.1 million to almost 1.8 million tons, as shown in Table 6.3. The major producing country is China, which accounted for almost 50% in 2010. Other major producers are Brazil, Norway, the United States, and France. These five countries account for more than 80% of the world's silicon production. The remaining 20% is covered by countries that have a minor production, such as Australia, Canada, Germany, Russia, South Africa, and Spain. Roskill (2011) reported that the four companies producing the most silicon were Ferroatlantica, Dow Corning, Elkem Bluestar, and Globe Specialty Metals.

TABLE 6.3 The World Production of Silicon, Thousand Tons (based on data obtained by Roskill, 2011)

	2001	2002	2003	2004	2005	2006	2007	2008	2009	2010
Australia	32	32	32	32	32	32	32	32	32	32
Bosnia-Herz.	—	—	2	3	8	16	13	13	11	16
Brazil	112	133	181	220	229	226	225	220	154	240
Canada	30	35	40	40	40	40	40	40	24	47
China	400	500	600	660	650	730	820	820	780	820
France	90	85	85	85	85	100	120	118	90	125
Germany	28	25	28	29	29	30	29	29	28	30
Laos	—	—	—	—	—	—	1	3	7	10
Norway	135	153	207	193	179	150	145	160	110	160
Russia	70	70	65	65	58	60	55	61	18	46
South Africa	39	43	49	51	54	50	50	49	51	50
Spain	30	27	28	25	35	32	32	33	15	30
Ukraine	5	5	8	8	8	8	5	5	5	5
United States	131	108	134	144	143	148	150	150	130	150
Total	1102	1216	1459	1555	1550	1622	1717	1733	1455	1761

TABLE 6.4 Composition of Metallurgical Silicon

	wt. %, max (except for silicon)				
Grade	Si	Fe	Al	Ca	Fe+Al+Ca
Si99	99	0.4	0.4	0.4	1
Si98	98	0.7	0.7	0.6	2
Si97	97	1	1.2	0.8	3
Si96	96	1.5	1.5	1.5	4

Some typical compositions of metallurgical silicon are shown in Table 6.4, and typical compositions of ferrosilicon are shown in Table 6.5. Note that practical compositions of commercial alloys, especially for minor impurities, may vary depending on the types and purity of the raw materials used. Some producers might require higher standards if the raw materials and processes allow so.

TABLE 6.5 Composition of Ferrosilicon (maximal content for all elements except Si and Al), balance—iron

	wt. %							
FeSi Type	Si	Al	P	S	C	Mn	Cr	Ti
FeSi10	8–13	<0.2	0.15	0.06	2	3	0.8	0.3
FeSi15	14–20	<1			1.5	1.5		
FeSi25	20–30	<1.5			1	1		
FeSi45	41–47	<2	0.05	0.05	0.2	1	0.5	0.3
FeSi50	47–51	<1.5		0.05		0.8	0.5	
FeSi65	63–68	<2		0.04		0.4	0.4	
FeSi75Al1	72–80	<1	0.05	0.04	0.15	0.5	0.3	0.2
FeSi75A11.5		1–1.5					0.3	
FeSi75Al2		1–2			0.2		0.3	0.3
FeSi75Al3		2–3					0.5	
FeSi90Al1	87–95	<1.5	0.04	0.04	0.15	0.5	0.2	0.3
FeSi90Al2		1.5–3					0.2	

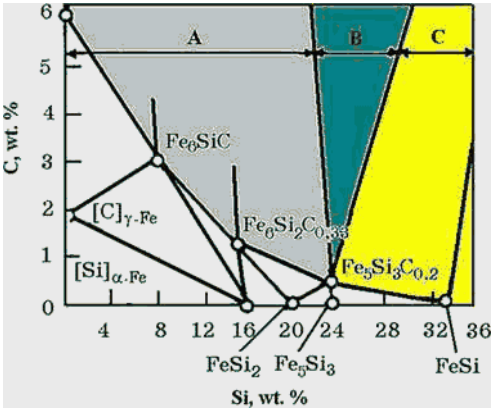

FIGURE 6.10 Influence of silicon concentration on carbon solubility in Fe-Si-C alloys at 1760°C. Excess solid phases in equilibrium with the melt are graphite (zone A), SiC (zone C), or both (zone B).

In the Fe-Si-C system, the solubility of carbon depends on temperature and silicon content, decreasing with higher silicon concentrations. Until ~24% wt. Si carbon solubility in melts decreases almost linearly. Iron, silicon, and carbon are able to form complex silicocarbides (Nowotny's phases) $Fe_xSi_yC_z$, where composition depends on the ferrosilicon grade. When carbon solubility is exceeded, the melt will be in equilibrium with graphite (zone A), graphite and SiC (zone B), or SiC (zone C) (Fig. 6.10). Thus, higher FeSi grades have much less carbon than low Si grades.

At high temperatures, both carbon and silicon dissolve well in iron, but on cooling excess phase (C or SiC) precipitates from the melt. To avoid fine graphite (<22% Si) or SiC (>24% Si) inclusions inside the ferrosilicon, the alloy is held in the ladle before casting.

Ferrosilicon (especially with lower Si content) may be granulated by pouring a controlled molten stream of alloy into a tank of water. The resulting granule size ranges from 0.2 to 2 mm. Low Si grades (<20% to 25% Si) are magnetic, which is an advantage in handling. These are used primarily as furnace blocks and are added in the form of controlled-weight piglets for initial deoxidization (Vishu et al., 2005). This type is also furnished in powder form for ore beneficiation (flotation in heavy suspensions). High aluminum ferrosilicon is used for the production of spheroidal gray iron to control and minimize the formation of carbides and decrease section sensitivity by refining graphite size and distribution. In ductile iron it is also known to be effective in minimizing carbide formation while increasing nodule count (Vishu et al., 2005).

6.3 SILICON AND FERROSILICON SMELTING TECHNOLOGY

6.3.1 Basic Principles of Operation

Silicon and ferrosilicon are produced carbothermally in electric arc furnaces. The major difference between silicon production and ferrosilicon production is,

of course, the presence or absence of iron in the system. Iron lowers the activity of silicon in the metal; hence, the major difference will be that ferrosilicon can be produced at a lower temperature, the Si yield will be higher, and the power consumption per ton of metal will be lower. However, the chemical reactions and the zones in the furnace are believed to be similar in the two processes, although for low Si ferrosilicon there will, of course, be additional differences.

Although the production is relatively simple in principle, the industrial process, which needs to be safe, environmentally sound, and effective, is much more complicated. As a high temperature is needed for production, silicon is produced in electric melting furnaces. This is the heart of the smelting plant. As shown in Figure 6.11, the plant consists of the following production units in addition to the furnace:

1. The mix unit where the raw materials are weighed and mixed before they enter the raw material silos.
2. The electrical system giving energy to the furnace
3. The off-gas units that cool down and remove the off-gas from the furnace
4. The processing units where produced liquid silicon is refined cast and crushed. These parts of the plant are often referred to as the downstream units or post tap hole units, as they come after the furnace—that is after the tap hole—in the value chain.

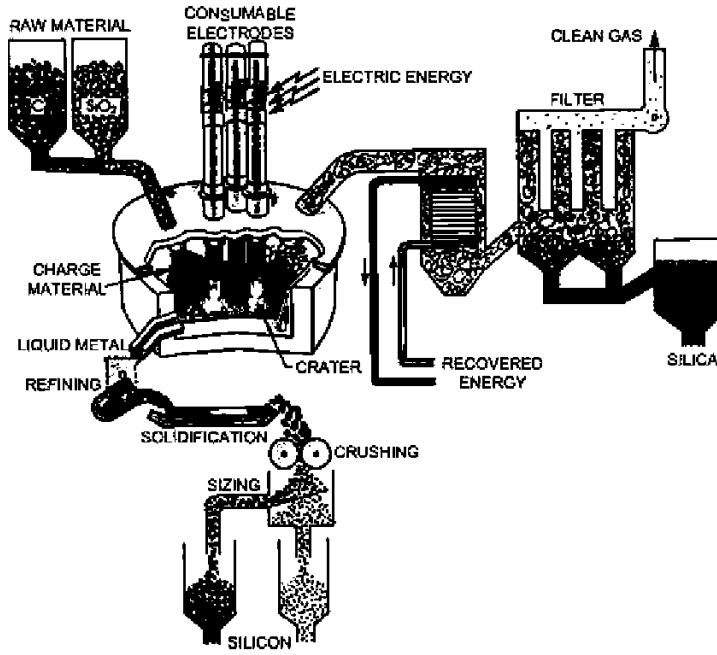

FIGURE 6.11 The schematic of the silicon smelting plant process. *(From Schei et al., 1998.)*

The electric energy is fed into the furnace through three electrodes, which are slowly consumed during production. In ferrosilicon smelting, electrodes are usually of the self-baked, Söderberg type, which are continuously replaced. Chapter 4 provides more details about self-baked electrodes technology. As they contain a steel shell that dissolves in metal, self-backed electrodes cannot be used in pure silicon production and prebaked electrodes are applied. For large-scale silicon furnaces, a composite electrode has been developed. These electrodes are made with a graphite core to secure the strength of the electrode. On the outer part, the less expensive carbon paste is used. The electrode is "extruded" through a steel casing to avoid adding iron to the silicon.

The off-gas plants consist of a cooler and a dust filter. Some plants also include an energy recovery unit. As energy is one of the main resources defining the profitability and sustainability of a process, energy recovery is expected to be a vital part of all plants in the future. From the furnace the gas species are mainly CO and SiO gas, and when these gases meet the air above the charge, they will exothermically oxidize to CO_2 gas and solid SiO_2. These reactions heat the fresh raw materials, keeping the temperature on top of the furnace between 700° and 1300°C. A higher temperature of the off-gas provides better energy recovery efficiency.

When the SiO-rich gas is oxidized, it forms "silica fume" or microsilica, consisting of solid, almost spherical SiO_2 particles, with an average size of only ~0.15 μm. In addition to the silicon, microsilica is an important by-product, which is used in the cement industry. The microsilica increases the strength and lifetime of the concrete. As an example, to strengthen the concrete in one of the highest buildings in the world, the Petronas Twin Towers in Kuala Lumpur, Malaysia, the Norwegian ferrosilicon company Finnfjord delivered about 4800 ton of microsilica.

Silicon is produced at temperatures above 1800°C in the furnace, so it stays in liquid form. The molten silicon is tapped into ladles. While the silicon is still liquid, the impurities less noble than silicon (Al, Ca, etc.) can be removed in an oxygen refining process to the form of oxides (slag). This is done by bubbling oxygen or air through the molten silicon. Silicon may also be oxidized, and the extent of the silicon oxidation is controlled by the rate of oxygen addition. However, if very small amounts of CaO and Al_2O_3 are present, the oxides will form inclusions (particles) in the molten silicon and do not actively move to form a separate slag phase. To prevent this, a flux $CaO\text{-}SiO_2$ is added to absorb the oxides. The oxide layer, whose density depends on the slag composition, will form on either the top or the bottom of the liquid silicon.

After the refining process, the liquid silicon is cooled and solidified. One typical method is to cast the silicon in big beds lined with solid silicon fines. This will prevent the silicon from being contaminated by other lining materials. When the silicon has solidified, it is crushed to a more convenient size. Some plants also granulate parts of the production by very gently pouring the liquid

silicon into a water pool. The product is thereby transformed into granules of a more homogeneous size. Liquid silicon in water has the potential to create violent explosions; hence, the granulation plant is situated in bunkers, which restrict the formation and possible direction of the explosion gases.

One of the important parameters controlled and adjusted by the furnace personnel is the submersion depth of electrodes. It depends also on the voltage switch and changes in the composition of the charge feed. Excess carbon reductant in the charge reduces the electrical resistance, so the depth of immersion of the electrodes in the charge decreases. A lack of reductant leads to an increase of electrical resistance and moves the electrode down (i.e., to deeper submersion). Significant deviations in the depth of immersion of the electrodes are a clear evidence of abnormal furnace operation, requiring charges in voltage steps or in the charge composition (Zubov and Gasik, 2002).

Typical symptoms of insufficient reductant in the charge are electrical current oscillations, unstable position of the electrodes in the charge, gas emission concentrated near the electrodes, increase of the charge sintering and number of gas fistulas, tapping of viscous slag, and partial furnace gases escape through the tapping hole. These lead to the thinning of the diameter and length of the working tip of the electrodes and an increase in the top charge temperature from 500°–600° to 1000°–1200°C with an increase in silicon losses due to SiO and dust. Delayed actions would cause a suspension of slag tapping and difficulties in closing the tap hole. The process might be restored by adding a "light" charge portion (with excess carbon reductant) under electrodes and by adjusting the operating voltage step.

Typical symptoms of reductant excess in the charge are rising of electrodes, narrowing of the crucibles (craters), avalanches of charge around the electrodes, sounds of electric arcs, difficulties in slag, and alloy tapping due to high SiC content. These symptoms might be caused by violations on short electrodes. Another cause is operation on electrodes that are too short (Shkirmontov, 2009a and 2009b).

Signs of good silicon/ferrosilicon furnace operation progress are (1) uniformly charge flow in all areas, without zones of over-sintered charge; (2) a deep position of electrodes; (3) positive gas pressure; (4) optimal temperature on the charge top (for ferrosilicon this could be below 500° to 600°C); (5) hydrogen content of the off-gas <5%, oxygen <1%; and (6) a constant off-gas flow rate. Too-high gas pressure is often due to a lack of reducing agent and the formation of large quantities of SiO (Gasik et al., 2011).

6.3.2 Smelting Process

6.3.2.1 Reactions in the Furnace

The core of the production process is the melting furnace. The furnace in general consists of a steel casing, lined on the inside with a material that can withstand high temperatures, mechanical stress when raw materials move

continuously through the furnace, and chemical wear when molten oxides/metals flow through it (Chapter 4 provides more details of furnace design, and Chapter 5 explores their electrical operation principles).

Electrical energy is fed into the process through electrodes. In AC furnaces for silicon and ferrosilicon smelting, the electric current flows from one electrode, through a gas cavity, down into the liquid bath, and up the next electrode. The gas cavity is formed around the electrodes' tip, and there an electric arc is ignited. The arc itself is a high-temperature plasma, up to 20 000 K, and is the source of heating in the arc furnace, increasing the temperature of the charge materials to 1800° to 2000°C. The DC closed furnace technology for smelting silicon has also been demonstrated, and significant effort has been put into its development (Vishu et al., 2005).

Most furnaces are semiclosed, which means the furnace has a partly open hood above the furnace chamber. The advantage of such a furnace is that one has access to the materials in the furnace through big hatches. An important part of the furnace operation is shifting the material to the high-temperature areas in the furnace, called stoking. In the silicon furnace, the production of condensates in the upper part of the burden is important to obtain a high silicon yield. However, the same condensate glues the charge and prevents a natural descent in the furnace. The stoking of the charge is thus an important part of the furnace's operation. Some industrial furnaces are also divided horizontally in the middle where one part rotates. This also contributes to a better raw material descent in the furnace.

The formal brutto-reaction of silicon reduction from silica is $SiO_2 + 2C = Si + 2CO$, but as shown previously, formation of SiO gas and solid SiC has a large influence on the whole process. In the furnace, raw materials are added from the top at ambient temperature and are quickly heated to 700° to 1300°C by the rising hot gas that burns at the top of the furnace. The raw charge materials are mainly SiO_2 and carbon. According to the equilibrium, SiO_2 will start to react with C to form SiC above 1500°C. Two solid particles of silica and carbon share only a small contact surface, and they will react with each other very slowly unless they were preliminarily mixed and supplied as briquettes or pellets.

From the high temperature area of the furnace, SiO gas rises to the cooler top area, where it reacts with carbon $SiO(g) + 2C = SiC + CO(g)$. This reaction is very important, because otherwise SiO gas will leave the furnace through the exhaust system and will oxidize to silica fume. The formation of SiO needs substantial energy, and if a lot of SiO gas leaves the furnace, the silicon yield is low and the power consumption becomes very high. If the residence time of SiO gas is long enough, even in the areas without carbon it will be disproportionate to silica and silicon ("condensates"): $2SiO(g) = Si + SiO_2$.

The materials that now sink down through the furnace into the high temperature area will consist of SiO_2, C, SiC, and some Si. Pure silica melts at 1723°C forming a viscous liquid. In the high temperature area (~2000°C), the

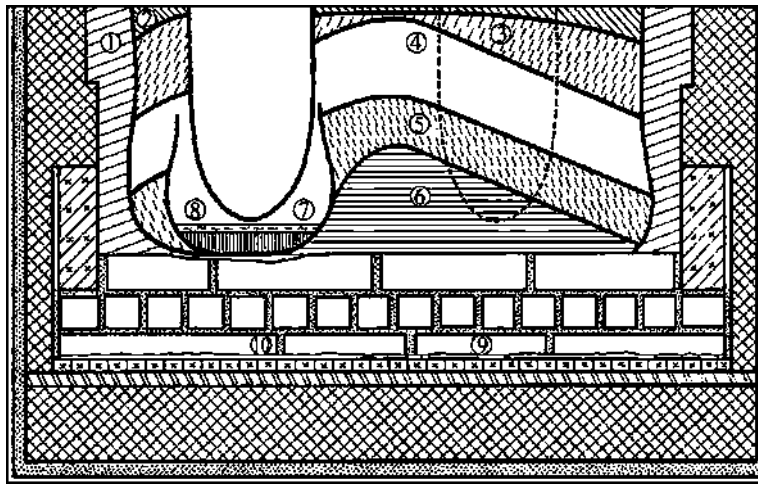

FIGURE 6.12 Cross section of the excavated open arc furnace after smelting silicon: 1, frozen lining; 2, sintered charge; 3, partially molten charge; 4, partially metallic charge; 5, molten and metallized charge; 6, SiC-rich crust; 7, silicon melt; 8, slag; 9, glassy phase; 10, slag penetrated under carbon bricks lining.

total process (unbalanced) may be described as $SiO_2 + SiC + C \rightarrow Si + SiO(g) + CO(g)$. It is important not to add too much carbon into the process zone as extra SiC will be formed and it may accumulate in the furnace ("freezing"). Figure 6.12 illustrates the results of the excavation of the industrial 16.5 MVA, silicon smelting furnace (Gasik and Gasik, 2011), indicating the main observed zones.

The mixture of SiO_2, SiC, and condensate behave as a bridge, stopping the further descent of raw materials. Below this region it will therefore develop a void around the electrode. In the bottom of this void, there will be a liquid silicon pool containing SiC particles. From the bridge of liquid SiO_2, drops of SiO_2 will fall down in the pool and react with SiC to form liquid Si and SiO gas. Heat is generated from electric current forming an arc between the electrode and the liquid silicon pool. In the cavity, a slight overpressure of 1 to 1.04 atm is measured (Kadkhodabeigi et al., 2011). When there is overpressure, internal avalanches and gas channels may be formed, leading to high off-gas temperatures and high SiO content. The temperature of the top of the charge could be as high as 1300°C, but it is very dependent on how much SiO will be condensed to Si and SiO_2 (Ringdalen and Tangstad, 2012).

Laboratory experiments have found that the rate of SiO formation from SiO_2 and SiC is more than two to three times faster than the $Si + SiO_2 \rightarrow 2SiO(g)$ reaction. If the contact area between the reactants changes dramatically, this may, of course, change the SiO production rates in the industrial furnaces. At lower furnace levels, SiO will mostly condense to a brown condensate (SiO_2 and Si) (Fig. 6.13).

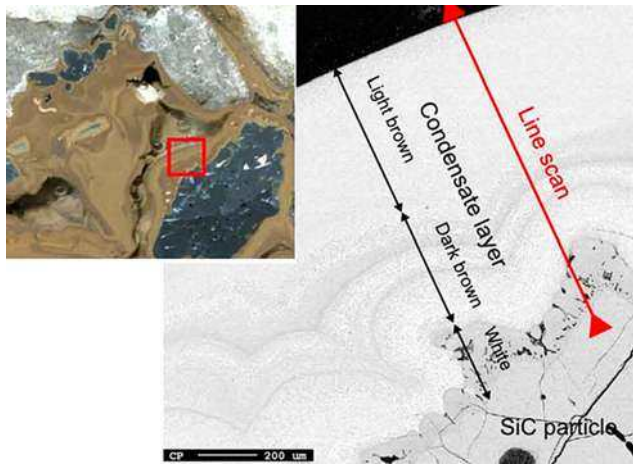

FIGURE 6.13 Macroscopic and microscopic views of condensate produced in a 50-kVA induction furnace.

This brown condensate may have various colors based on the size of the spherical silicon particles, and larger Si spheres give a darker color. A thin white condensate layer might be observed covering these particles (see Fig. 6.13), and its composition is $SiC + SiO_2$ coming from the reaction of SiO and CO in the gas phase. White condensate is believed to form when the temperature and SiO pressure are lower than they are for the formation of brown condensate. As the brown condensate is heated, silicon particles will coalescence into larger drops and leave the condensate area when the temperature exceeds the melting temperature of quartz.

Laboratory experiments show that condensate from SiO gas will create a layer that can hold the weight of the charge located above, and thus create a cavity. So the formation of the cavity due to SiO condensation is important in addition to the crater formed around the electric arc (Myrhaug, 2003).

The previous excavation of an industrial ferrosilicon furnace showed only one large crater around each electrode (Schei et al., 1998). However, in the more recent industrial excavation (Ringdalen and Tangstad, 2012) the layers of condensate outside the SiC crater wall were also found in addition to a condensate layer between the charge mixture and the crater. These layers could have been formed by SiO gas from the crater, which flowed from the bottom and outside the crater walls. They contribute to building up the crater and may also be of importance for the rate of the reactions that take place. The SiO condensation can take place close to the crater walls where the estimated temperature is 2000°C. Of note, two cavities, one for the arc crater and one built up by condensate, can be found in even larger furnaces or furnaces with other temperature distributions.

In small furnace experiments, the condensate cavity was found to grow downward from the position of the condensation temperature. This contradicts that described in earlier studies (Schei et al., 1998), where the cavity was believed to grow outward from the consumption of materials around the electrode tip. After the stoking process, where the materials are mechanically pushed into the cavity, both mechanisms may contribute to the cavity formation; a new charge roof will form due to condensate formation, and the materials below this condensate roof will be consumed by the arc from the electrode tip.

6.3.2.2 Peculiarities of Ferrosilicon Smelting

Ferrosilicon is usually smelted in closed submerged arc furnaces with power of 22 to 93 MVA (Fig. 6.14); example parameters are shown in Table 6.6 (Gasik and Gasik, 2011).

The silica source for producing ferrosilicon is usually quartzites of lump size 20 to 80 mm, subjected to prewashing, crushing, and grading if needed. Quartzites suitable for smelting of ferrosilicon must contain not less than 97% SiO_2 and not more than 1.5% Al_2O_3. The carbon reductant is usually nut-coke of 5 to 20 mm in size, but as mentioned previously, different producers may have their own local reductant recipes. The reductant should possess high electrical resistance and high reactivity in relation to SiO_2 and SiO reduction, and constant moisture content (Batra, 2003). Approximate charge composition, energy demand, and silicon yield for ferrosilicon smelting in closed furnaces are shown in Table 6.7 (Gasik et al., 2011).

The presence of iron during the carbothermic reduction of quartzite lowers the partial pressure of SiO required for reduction to silicon and reduces its activity due to the formation of Fe-Si solutions. Thus, the losses of SiO from the furnace top decrease as the iron content of ferrosilicon increases, so it is typical to have silicon recovery of greater than 90% to 95% for $<$50% Si grades of ferrosilicon (Vishu et al., 2005).

Ferrosilicon production is a nearly slag-free process (the silicate-based slag amount does not exceed 3% to 5% of the alloy mass). However, the tapping of ferrosilicon and slag through one tap hole might be complicated by changes in the slag composition. The slag is heterogeneous, consisting of silicate-based melts (48% to 50% SiO_2, 20% to 25% Al_2O_3, 15% to 18% CaO), suspension of silicon carbide (10% to 15%), and the metallic inclusions of ferrosilicon alloy. Silicate component is formed from silica and impurity oxides (Al_2O_3, CaO, MgO) contained in quartzite and coke ash. Silicon carbide forms as an intermediate product of silica reduction by carbon, as shown earlier. Depending on the silicate melt chemical composition, the slag can be solidified in different concentration fields of anorthite ($CaO \cdot Al_2O_3 \cdot 2SiO_2$, melting point 1553°C) and gehlenite ($2CaO \cdot Al_2O_3 \cdot SiO_2$, melting point 1545°C) of the CaO-Al_2O_3-SiO_2 system (Fig. 6.15).

Anorthite-area compositions, including the presence of SiC particles, have higher viscosity and a lower ability to separate from metal. Therefore, lime is

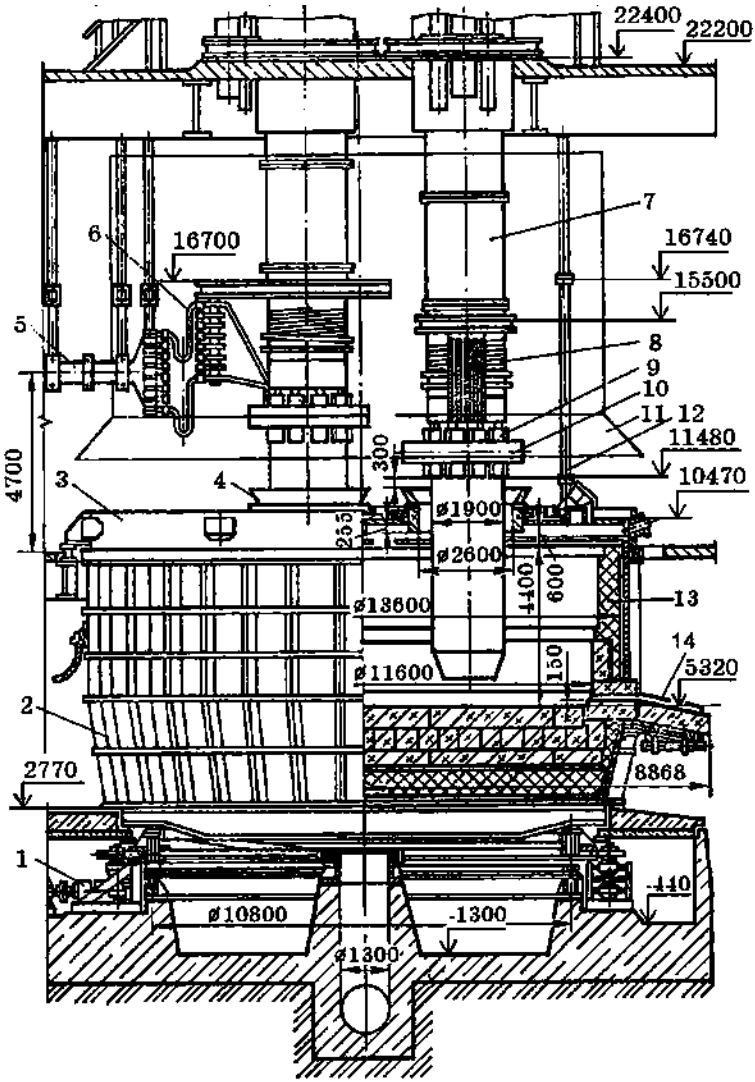

FIGURE 6.14 Round hearth 63 MVA power furnace: 1, mechanism of furnace rotation; 2, furnace shell; 3, arc furnace; 4, feeding funnel; 5, short net; 6, short net flexible bus bars; 7, electrode holders; 8, secondary current leads; 9, electrode contacts; 10, pressure ring; 11, furnace hood; 12, suspension; 13, refractory lining; 14, tap hole.

periodically added to increase basicity and to move slag composition into the gehlenite area.

Ringdalen and Tangstad (2012) reported the results of the excavation of an industrial ferrosilicon furnace (Fig. 6.16). They confirmed the existence of one large cavity around each electrode with walls made up of SiC and small

TABLE 6.6 Examples of the Furnace Parameters for Smelting Ferrosilicon

Parameters	Furnace A	Furnace B	Furnace C
Furnace power, MVA	27	40	80
Hearth depth, mm	2900	3500	5000
Hearth diameter, mm	6800	8700	11 600
Electrodes diameter, mm	1400	1500	1900
Electrodes current, kA	85	103	172
Power factor cos(φ) (with compensation)	0.93–0.94	0.91–0.92	0.89–0.90
Electrical efficiency	0.91	0.915	0.89

TABLE 6.7 Typical Materials and Energy Demand for Smelting of Ferrosilicon in Closed Furnaces (per one basis ton of alloy)

FeSi Alloy	FeSi20	FeSi25	FeSi45	FeSi65	FeSi75Al1
Quartzite, kg	370	552	931	1568	1930
Iron chips, kg	810	780	658	343	250
Coke, kg	200	280	438	720	845
Electrode paste, kg	10	8	16	43.3	54
Electric energy, MWh/t	2.1	2.7	4.8	7.4	8.8
Silicon yield, %	94–95	97–98.5	98–99	92–94	91–93

amounts of quartz. Several gas channels existed within the walls, creating a layered structure. The channels started at the bottom of the crater, where they were widest. The gas flow appeared to move from the bottom of the crater, through the channels, up to the charge material.

Condensate occurred both in vertical layers outside the crater walls and in a horizontal layer high up through the furnace. Lumpy silica was found only in the upper 20 cm of the charge mixture and below this, the silica component was generally disintegrated. Most of the silica phase was transformed from quartz to cristobalite (Ringdalen and Tangstad, 2012).

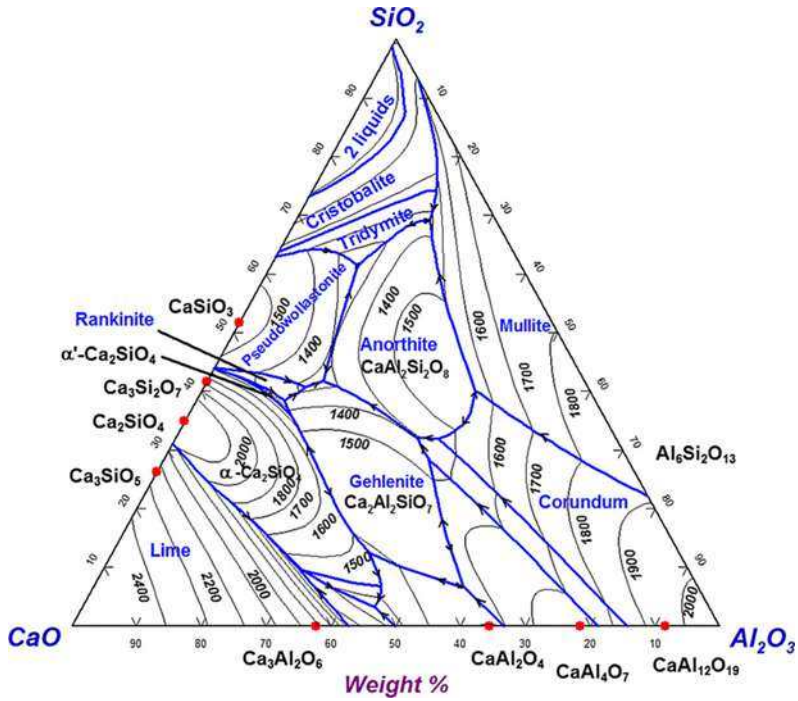

FIGURE 6.15 Diagram of phase equilibria (liquidus projection) in the system CaO-Al_2O_3-SiO_2. Solid lines, boundaries of coexisting mineral phases; thin lines, isotherms (calculated with FactSAGE 6.2).

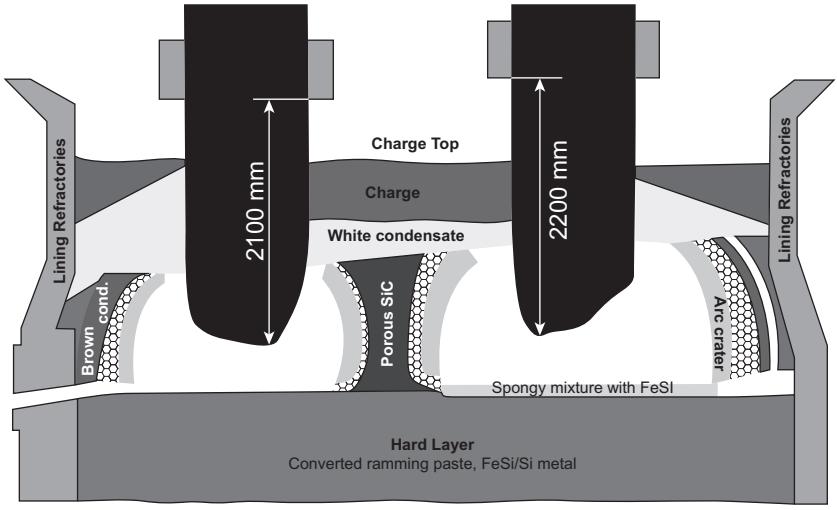

FIGURE 6.16 The distribution of material during the excavation of an industrial FeSi furnace of 7 m diameter. *(Ringdalen and Tangstad, 2012).*

6.3.2.3 Silicon Yield, Energy Demand, and Costs

The silicon yield (i.e., the ratio of silicon tapped from the furnace to the silicon added into the furnace) can be described as follows:

$$\text{Si yield} = \frac{\text{Mass Si tapped}}{\text{Mass Si tapped} + \text{Mass Si in SiO leaving the furnace} + \text{Mass of Si in accumulated SiC}}.$$

In balanced operated silicon smelting, the accumulation of SiC in the furnace will be close to zero and it is a valid assumption for some time. Hence, the Si yield will first of all depend on how much silicon is produced (reduced) in the high temperature zone, and second, will depend on how much of the SiO gas can be captured in the low temperature part of the furnace.

In an ideal case with 100% Si yield, no SiO gas leaves the furnace and no SiC is accumulated. The theoretical enthalpy change to heat up silica and carbon from ambient temperature to produce silicon melt at 1800°C and CO gas at 1000°C would be 9.854 MWh/t Si. If the silicon yield is zero, which means all silicon is lost as SiO gas at 1000°C, this value would be 9.01 to 9.02 MWh/t Si. Thus, energy required for the process is inversely proportional to the Si yield (Fig. 6.17).

The Si yield has a significant effect on both the used electric energy costs as well as the fixed costs. With a lower energy consumption per ton of silicon produced, the tonnage will increase with a given furnace capacity in MVA.

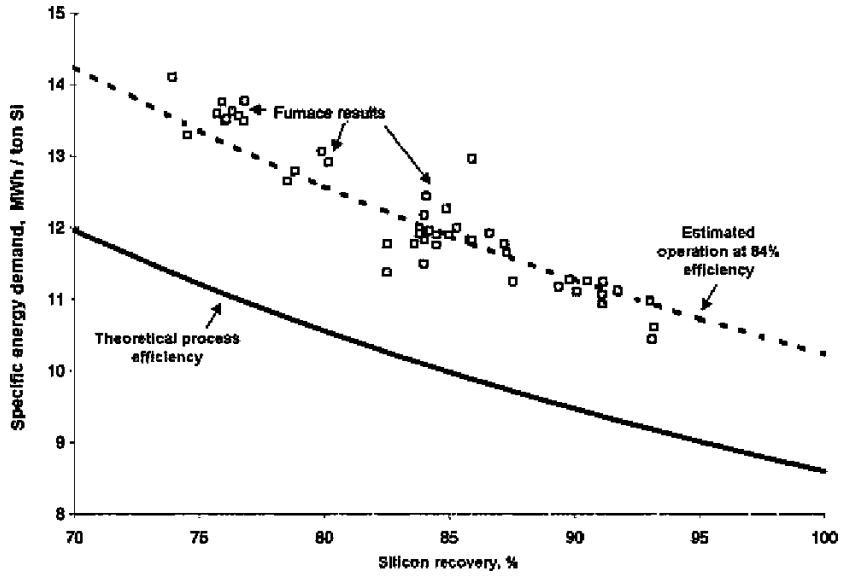

FIGURE 6.17 Measured and calculated energy demand for silicon production. Dashed line was fit with an assumption of energy efficiency of 84%. *(Data from Schei et al., 1998.)*

These numbers are, of course, very dependent on the individual raw material prices in each of the countries where the silicon is produced. However, changes in Si yield will affect the cost almost linearly in any case.

The most important factors affecting the Si-yield in the furnace were identified by Schei et al. (1998) as temperature in the cavity, SiO reactivity of the carbon reductant materials, and temperature in the low temperature zone. If the high temperature zone is "cold" (~1800°C), the SiO partial pressure is high and the silicon yield will be low (33%), as most of it will be recirculated in the furnace reducing from SiO to SiC and back. If the high temperature zone is "hot" (1950° to 2000°C), the partial pressure of SiO is closer to CO, which fits better the stoichiometry of the process, leading to nearly theoretical 100% silicon yield. This shows that it is important to obtain a high temperature in the high temperature zone, to therefore obtain a low SiO pressure to produce the same amount of silicon.

In the preceding example, it was assumed that all C in the low temperature zone was reacted to SiC. However, this reaction extent is determined in the furnace by kinetics. The rate is determined first by the distribution of the SiO gas in the burden (i.e., the permeability of the burden), second by the size of the carbon materials, and last by the reactivity of the carbon materials.

High carbon reactivity toward SiO gas is vital to obtain a high Si yield of the process. When this is high, the SiO gas is captured by the carbon in the upper regions of the furnace and will react according to the reaction: $SiO(g) + 2C = SiC + CO(g)$. At these conditions very little SiO gas will escape from the furnace at equlibrium (<1% as shown by Fig. 6.5). However, the practical limitations of the reaction due to kinetics dictate these losses typically at about 10% to 20%.

The reaction $2\,SiO(g) = Si + SiO_2$ also catches a lot of SiO gas produced in the high-temperature zone, and this reaction is directly affected by the temperature and condensation area. To obtain a high rate of the condensation reaction, the gas has to be evenly distributed in a charge with as low a temperature as possible.

The bigger the void around the electrode, the smaller the distance between the void and the top of the charge. A small zone for the preliminary reactions leads to less reaction of SiO gas with the carbon materials. This is due to a high temperature on the surface and because of a low number of carbon particles for the gas to react with. At regular intervals, the furnace is therefore stoked (i.e., a new, cold charge is mechanically forced into the void to collapse it). This treatment of the oven is necessary to reduce the SiO loss.

An increase in the carbon content of the charge will capture more silicon, but at the same time generate more accumulated SiC in the bottom and edges of the furnace. This will eventually lead to SiC buildup in the furnace. The electric energy is then developing heat higher up in the furnace, which is a problem, as shown earlier for abnormal ferrosilicon operations. In the worst case, the furnace has to be stopped in order to remove the SiC-buildup. The optimum

carbon addition will give the highest Si-yield and hence the lowest energy consumption.

6.4 CASTING AND REFINING OPERATIONS

6.4.1 Casting

Unlike the methods used for iron and steel castings, similar procedures for silicon and ferrosilicon require much more care and development. Besides ferrosilicon, which is usually used almost exclusively for steelmaking, silicon has a wider range of applications (aluminum alloys, chemical industry, electronics, etc.), which dictates different quality requirements in chemical composition (impurities—trace elements) and grain size (especially fines).

Silicon going to the chemical industry ends up in a bed requiring a sizing between 100 and 200 μm where the silicon reacts with chemical agents. This is a surface reaction and hence elements catalyzing/retarding this reaction are of importance. The quality of the silicon will also affect the reaction rate. Some phases do not react, and hence the selectivity of the material also varies. In particular, phases containing Fe, Al, and Ca give a low selectivity and are thus not desired. Besides total content of trace elements, their distribution on grain boundaries versus solution in the Si crystals is important.

The total number of fines, as this particularly affects the total oxygen content in the metal, is the next critical issue. The number of fines formed depends on the strength of silicon, which again is dependent on phases in the metal and their grain size. For conventional diffusion-driven solidification, the grain size is proportional to the inverse cubic power of time, as shown by Schei et al. (1998).

Homogeneity of the metal regarding both element distribution and phase distribution is critical. Although the liquid Si/FeSi has a homogeneous distribution of trace elements, they will segregate during solidification due to their partition ratios (segregation coefficients) between solid and liquid phases. The solubility of the elements is in most cases lower in the solid phase than in the liquid phase. When the first part of the melt starts to solidify, the initial trace element content will be very low in the solid phase; hence, its content in the liquid phase will increase. As more of the slab is solidified, the content in the liquid phase gradually increases. The recently solidified part will be in equilibrium with this high content liquid, so the content in the solid phase will increase as the solidification proceeds. Within this formalism, the trace element content in the solid (C_s) will depend on the fraction already solidified (f_s), the specific segregation coefficient k_o, and the initial trace element content (C_0) according to the Gulliver-Scheills equation:

$$C_s = k_o C_0 (1 - f_s)^{(k_o - 1)}$$

TABLE 6.8 The Segregation Coefficient k_o of Some Elements in Silicon

Al	$2\cdot10^{-3}$–$2.8\cdot10^{-3}$	Cu	$4\cdot10^{-4}$–$8\cdot10^{-4}$	P	0.35
B	0.8	Fe	$6.4\cdot10^{-6}$–$6\cdot10^{-5}$	Sn	0.016
C	0.05–0.07	N	$7\cdot10^{-4}$	Ti	$2\cdot10^{-6}$–$3.6\cdot10^{-4}$
Ca	$8\cdot10^{-3}$	Ni	$8\cdot10^{-6}$–$3\cdot10^{-5}$	Zn	$1\cdot10^{-5}$
Cr	$1.1\cdot10^{-5}$	O	0.25–1.4		

The segregation coefficients for metals are usually very low as shown in Table 6.8, whereas for elements like C, O, B, and P they are in the order of unity. This means the same content of these trace elements will be in the solid and in the liquid phase, so the content should be similar throughout the cast product.

However, the solidification direction during casting of metallurgical grade Si and FeSi is usually not fixed, so the distribution of trace elements might not be according to the ideal state of Gulliver-Schell's equation. The practice shows that the distribution of trace elements may vary with a factor of 5 through the silicon ingot, and the slower the solidification, the larger the variation in trace element content. Among the casting and atomizing methods investigated for silicon solidification, many options have been developed and tested (Table 6.9).

Processes for casting ferrosilicon are quite similar to those used for silicon. During solidification of the standard grade of 75% ferrosilicon, silicon crystallizes initially, followed by solidification of the ε-phase. The transformation of the ε-phase to stable $FeSi_2$ is accompanied by an increase in volume, which can lead to disintegration of the alloy in the range of 45% to 65% Si alloy (Vishu et al., 2005). The microstructure of FeSi45 alloy has FeSi phase, non-stoichiometric Fe_xSi_2, and that of FeSi65 extends to Fe_xSi_2 phase and pure silicon. Trace elements may form excess phases, which have a complex chemical composition. They are usually crystallized at the grain boundaries of iron silicides (Zubov and Gasik, 2002).

Substandard ferrosilicon fractions can be converted into commercial products by recycling them with the original charge in FeSi smelting furnaces, by briquetting, pelletizing, or remelting in induction furnaces. Some technologies have been developed and implemented for briquetting ferrosilicon fines.

6.4.2 Refining of Silicon and Ferrosilicon

6.4.2.1 Trace Elements Distribution

The feed materials going into a furnace are carbon materials and quartz, both containing trace elements. These elements will be present in one of the three flows passing out of the furnace: metal, silica in the off-gas, and gas.

TABLE 6.9 Reported Methods of Silicon Casting and Atomizing (from Nygaard, 2006)

Method and Developer	Features
Atomizing in inert gas (Elkem Meraker); 800 t were produced in the pilot plant	Very high cooling rate and small particles that in principle can be used directly in the chemical industry. High productivity, but feasible product yield was not high; increased costs.
Air granulation (Fesil), forming ~1 mm bullet particles	The layer of oxidized silicon on each particle was high to develop further production.
Water granulation (Elkem, Fesil, Silicon Smelters, Becancour Silicon)	A number of crucial requirements that must be met to prevent explosions, but they cannot be avoided, so many producers have now stopped this method due to the instability of the process.
Cooling down in water sloping channel (Mintek); forming large lumps (4–8 × 20–50 mm diameter)	The sloping channel is filled with about 10 mm of water, allowing poured liquid metal to slide along the bottom and to form lumps. No full-scale process was reportedly built in a silicon plant.
"Cast to shape" in copper molds (Elkem trial).	The molds were rod-shaped, allowing rods to fall out and break up into pieces ~10 × 10 mm. This process was never introduced into production, and costs were too high.
Casting on flat copper plates (Becancour Canada, Ferroatlantica)	Rotating copper plates or flat copper plate in the bottom of a vibrating feeder. Oxygen content is believed to be very low; fines fraction is three times lower versus cast and crushed material.
Casting in cast iron molds	Silicon dissolves iron; volume expansion may create cracks in the molds, silicon fines must be used to protect the molds. However, it introduces a high amount of oxygen.
Multiple layer casting (first layer cast onto the bed of fines, subsequent one on top of the previous layer)	Probably the cheapest solidification method. Each layer is typically 5–15 cm. The effect of fines and oxygen is reduced versus the first layer. Not very rapid cooling as with other methods, but low cost.

Sometimes also smaller quantities of slag may be tapped together with the metal. Most of the impurities introduced into the furnace via the raw materials and any other sources are transferred to the product. Myrhaug (2003) has shown an example of the distribution of trace elements in silicon smelting (Fig. 6.18). Such partition figures, however, vary from furnace to furnace, but they reveal the major trends in elements distribution.

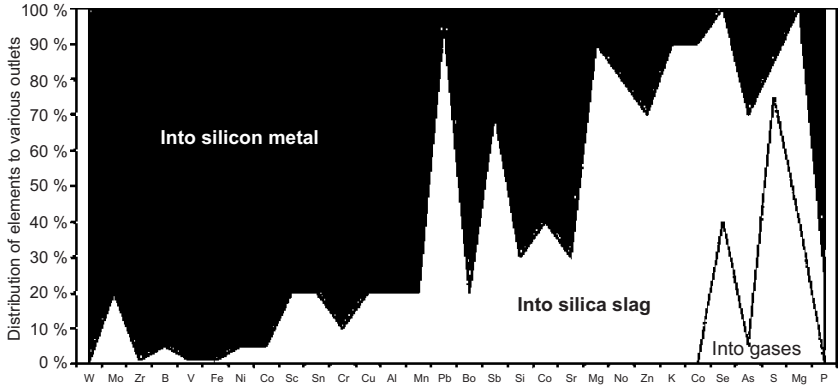

FIGURE 6.18 Example of a trace element partition between different products of silicon smelting. *(From Myrhaug, 2003.)*

Most trace elements follow the boiling-point model, which states that the elements with the lowest boiling temperature will go to the gas phase, the elements with a slightly higher boiling temperature will condense on the microsilica or stay in the slag, and the ones with the highest boiling points will mostly go into the metal. Some elements deviate from the boiling point model and vary significantly between measuring campaigns. As the trace element content is close to the analytical limits, it is believed that the deviation is mostly due to analytical inaccuracy at these low levels. To produce high purity grades of silicon and ferrosilicon, the tapped alloy is refined by different methods.

6.4.2.2 Refining Processes

Typical elements that must be controlled in silicon are Fe, Ca, and Al. As Ca and Al are less noble than Si (have higher oxygen affinity), they can be removed by oxidation. Iron, however, can only be controlled by limiting the Fe content in the raw material as in the quartz and the carbon reductant ash. For some grades, the content of oxygen and carbon can also be of importance. Ferrosilicon, titanium, and chromium might be also limited if their content in raw materials is initially high.

Oxygen for refining might be introduced as gas or air (blown from a lance or via a plug in the ladle) or as oxides (e.g., Fe_2O_3 in the case of ferrosilicon refining). In either case, thermodynamics is based on the reaction of dissolved Al and Ca with oxygen species, giving alumina or CaO, which is absorbed by the special slag phase. Due to the low content of impurities in the metal phase, slag composition and temperature are essential to provide the thermodynamic driving force for the reactions.

The equilibrium between the melt and slag is achieved when a certain amount of aluminum in the alloy is reached and alumina content in the slag $CaO\text{-}Al_2O_3\text{-}SiO_2$ (and its viscosity) is increased. Common slag compositions are based in the triangle $SiO_2\text{-}CaSiO_3\text{-}CaO\cdot Al_2O_3\cdot SiO_2$ (anorthite) (see

Fig. 6.15). Thus, to reach lower aluminium content, slag treatment might be repeated two or three times, but this leads to higher silicon losses and increased electrical energy consumption. To improve the refining procedure, slag may additionally have some CaO and CaF_2 as flux to reduce its viscosity, while blowing oxygen-containing gas into the melt. Although aluminum in this case is removed more efficiently, more silicon is also oxidized. There were also methods of refining ferrosilicon that involved applying mixtures of siderite ($FeCO_3$) with fluorspar. Siderite decomposes on heating to FeO (oxidizes aluminum) and CO_2 (provides gas for efficient mixing), whereas fluorspar decreases viscosity. As the final level of refining is dictated by the product specification, the result does not depend on the method used. However, the heat balance and the cost may, of course, be affected by the method preferred.

Oxygen and carbon are present in the metal only as ppm quantities, hence in the solidified product most of the carbon and oxygen are present as oxides and carbides (Tang et al., 2010). However, the total oxygen and carbon content is also higher than the liquid solubility given by the phase diagram, and hence it shows that, already at liquid state, the melt contains some oxides and carbides. Reported oxygen contents are between 0.04% and 0.70% (Schei et al., 1998). Oxygen is a specific concern for silicon used in the chemical industry. During refining, the use of viscous crusty oxide films (adding CaO or CaO with silicates) to activate the bottom slag should be avoided throughout the process, to avert "over-oxidation" and to add an inert gas that will keep gas bubbles from collapsing before reaching the slag layer. Operating at a high degree of turbulence and adding fluorspar at the end of the blow will help to keep the oxygen content low.

Contrary to silicon production, the oxygen solubility increases and the carbon solubility decreases when the iron content in FeSi is increased. When the metal is tapped from the furnace, the carbon content is assumed to be close to the solubility limit at these temperatures. As the temperature decreases during pouring, stirring, and casting, SiC (or graphite for alloys with $<22\%$ Si) will be precipitated. The resulting carbides end up in the lining and in the slag phase. As Al_2O_3-CaO-SiO_2 slags wet SiC well, slag additions are efficient to remove formed SiC particles from the metal.

The contamination of chemical-grade silicon with small amounts of the oxide slag was found to be detrimental to the silicon performance. Therefore, oxide slag must be removed from molten silicon by phase separation during casting. This can be improved by controlling the process to generate an oxide slag with suitable viscosity, density, and melting point (Vishu et al., 2005).

6.5 ENERGY SAVINGS AND ENVIRONMENTAL ISSUES IN SILICON AND FERROSILICON PRODUCTION

6.5.1 Energy Recovery

In energy balance calculations, the reference state is usually taken for the highest oxidation step of each element at 25°C. The energy flow going into the

furnace can be divided into several streams, namely electric energy and the latent energy contained in the charge materials. The electrical efficiency of the furnace versus the incoming energy on the transformer primary circuit is estimated as 85% to 90% depending on the furnace power and design. About one fourth of the electrical power loss is in the leads (bus bars) and transformers, and about half of the loss is in the electrodes. Solid carbon reductant brings into the process about 9 MWh/ton and coke volatiles bring in about 13.8 MWh/ton of CH_4, assuming volatiles are converted into methane.

The outcoming energy flow is divided into the following streams: energy in the off-gas, in the products like slag and metal; chemical energy plus latent heat at 1600°C; and energy removed with cooling water.

An example of the energy balance for a 10-MW furnace is shown in Table 6.10. The chemical energy flow is of the same order as the electrical energy input to the furnace, and about 85% of it is converted into the chemical energy of the products. As the temperature in the off-gas in a silicon furnace is high, half of the energy is in the off-gas as thermal energy. The gas on the top of the furnace contains CO_2, N_2, and unreacted O_2, in addition to the minor species like NO_x, SO_2, and so on.

The temperature in the off-gas is dependent on how much of the CO and SiO gas is oxidized and how much surplus air is in the off-gas. Usually all CO and SiO is oxidized to CO_2 and SiO_2(s). The temperature of the off-gas is calculated based on 1400°C for the gas coming from the charge and 80% Si recovery. If the air inlet is limited, the temperature can reach more than 2500°C. However, this is seldom the case and the temperature is usually much lower due to excess air that cools the off-gas. This is also important due to the temperature limitations in the filter bags.

There has been continuous development in the silicon industry to reduce energy consumption, especially by increasing the Si yield, and increase energy recovery by utilizing the energy in the hot water and making extra electricity

TABLE 6.10 Example of a 10-MW Silicon Smelting Furnace Energy Flow Balance (from Kamfjord, 2012)

Incoming Streams	MW	Outgoing streams	MW
Electricity	10	Smelting products	7.33
Solid carbon	8.41	Off-gas energy	11.14
Coke volatiles	3.28	Cooling water	2.87
		Other losses	0.34
Total in:	21.68	Total out:	21.68

from the high temperature off-gas flow. Hot water utilization depends on the country's conditions. For example, in Norway it is used to grow flowers, to produce fish, and to keep public areas free from snow.

Also, some plants recover the energy in the off-gas by producing electrical energy. From the off-gas share of 11.14 MW shown in Table 6.10, directed into the boiler, about 75% (8.35 MW) might be recovered as steam. When this steam is used to run a turbine and generator of total 25% efficiency, about 2 MW of electricity can be produced, which is 20% of the electric power consumed by the furnace originally. For hot water, about 90% of the electrical energy can be recovered.

The energy streams are dependent on the raw materials used and the operation of the furnace, so they naturally vary over time. For example, within 48 h of furnace operation, energy flow in the products and off-gas varies by about ±15% of the furnace effect. These variations have to be taken into account when designing energy recovery units.

6.5.2 Emissions Control

The emissions from a plant can be divided in two groups: controlled emissions and diffuse emissions. Controlled emissions of energy and materials are those going through the stack and other off-gas handling systems. Diffuse emissions of energy and materials are those that are not captured by the off-gas systems and hence are distributed randomly ("diffused") through the plant.

Controlled solid emissions from ferrosilicon production are mainly fines containing the off-gases. The precipitator's dust from dry gas cleaning has usually 80% to 95% SiO_2, 1.5% to 9% Al_2O_3, 0.4% to 2.7% CaO, 1% to 5% MgO, <0.5% Fe_2O_3, and <2% others. This dust, with an average particle size of 5 μm, has a very high specific area (~2000 m^2/g) and low bulk density (180 to 230 kg/m^3). It has been estimated that 10% to 15% of all silicon losses during the smelting of FeSi75 contains in these fines (Zubov and Gasik, 2002).

Determining the rational use of silica dust captured during gas cleaning is one of the urgent tasks in ferrosilicon production to save material resources and to improve the efficiency of environmental objectives. The principal health hazard is caused by the crystalline form of silica (quartz) used as a raw material, as it is the chief cause of disabling pulmonary fibrosis, such as silicosis (Vishu et al., 2005). Different methods of dust utilization are being studied, like the application in the cement for constructions and the preparation of "liquid glass" (sodium silicates) by an aqueous caustic treatment. This includes ceramics production, sorbents, manufacturing of silicon tetrachloride, abrasive SiC and Si_3N_4, and so on.

Diffuse or fugitive emissions occur wherever materials are exposed to handling. They may be solid materials, like raw materials and produced metal, or liquid metal. In the solid state, the fume will come from the abrasion of the

FIGURE 6.19 Examples of fugitive emissions from ladle before casting *(left)* and during tapping *(right)* *(Kamfjord, 2012)*.

solid material, whereas in the liquid state, evaporation will be the main source. Splashing may also contribute but is believed to be of minor significance.

The three main drivers for reducing diffuse emissions are to increase the health of the workers at the plant, to reduce the cost of production, and to reduce the environmental footprints of producing silicon and silicon alloys. Compared to the workers at FeMn and FeCr plants, the workers at Si/FeSi plants have reduced respiratory capacity with a factor of 2, and this is correlated to the work operations and earlier exposure. This was recognized a long time ago (Swensson et al., 1971) and many measures are being taken to quantify and to reduce the diffuse emissions. Typical examples of fugitive emissions are presented in Figure 6.19, which shows smoke from a ladle used during transport and tapping (Kamfjord, 2012). At every step—from raw materials handling to smelting and reduction, casting, and crushing—fume, dust, and energy are released to the surroundings.

In Table 6.11 these emissions have been quantified (Kamfjord, 2012). The two major pollution time periods are during casting and during tapping, but the leaks from the furnace process and the crushing, screening, and packing processes are also quite high.

During environmental monitoring campaigns in tapping and casting areas, the average dust load in the air was 6 to 12 mg/Nm^3; however, when the dust content was measured only in areas where it had been observed, the numbers were 23 to 45 mg/Nm^3 and 223 mg/Nm^3 outside of the tapping area and above the casting area, respectively. Therefore, it has been concluded that fugitive emissions occur mostly when ladles are transported in the plant after tapping

TABLE 6.11 Major Emissions in the Silicon Smelting Plant

Process Stage	Share of Diffusive Emissions, %	Share in Internal Pollution, %	Emission Type
Materials handling to storage	0–5	0	Fume—transportation, conveyers, etc.
Materials transport to furnace	0–5	5–10	Fume—mixing, transportation
Furnace processes	10–20	5–20	Smoke and fume—escaping from furnace gas system
Tapping	20–40	30–50	Smoke and fume—tapping
Casting	20–40	15–25	Smoke and fume—liquid metal handling
Crushing, screening, packing	5–15	5–15	Metallic fume
Off-gas systems	5–10	0–5	Fume and smoke escaping gas systems
Off-gas collected products packing	0–5	5–10	Fume—passage into work environment

and during the casting process, probably due to the purge gas stirring and refining operations. Intensive gas collection in suction hoods is therefore required over the ladles and in similar locations (Kamfjord, 2012).

REFERENCES

Aasly, K., 2006. Properties and behaviour of quartz for the silicon process. Ph.D. Thesis 236. NTNU, Trondheim, Norway, 187 pp.

Batra, N.K., 2003. Modelling of ferrosilicon smelting in submerged arc furnaces. Ironmaking & Steelmaking 30 (5), 399–404.

Gasik, M.I., Gasik, M.M., 2011. Electrothermal silicon technology. Dnipropetrovsk: National Metallurgical Academy of Ukraine, 487 pp.

Gasik, M.M., Gasik, M.I., 2010. Thermodynamic analysis of the dominant phase equilibria in M(Si, Cr, Al)-O-C systems. Russian Metallurgy (Metally) 6, 548–556.

Inoue, Z., Ueno, S., Tagai, T., Inomata, Y., 1971. A new polytype of silicon carbide 9T. Journal of Crystal Growth 8 (2), 179–183.

Kadkhodabeigi, M., Tveit, H., Johansen, S.T., 2011. Modeling the tapping process in submerged arc furnaces used in high silicon alloys production. ISIJ International 51 (2), 193–202.

Kamfjord, N.E., 2012. Mass and energy balances of the silicon process – Improved emission standards. Ph.D. Thesis 162. NTNU, Trondheim, Norway, 139 pp.

Myrhaug, E.H., 2003. Ph.D. Thesis 67. Non-fossil reduction materials in the silicon process – properties and behaviour. NTNU, Trondheim, Norway, 226 pp.

Myrvågnes, V., 2008. Analyses and characterization of fossil carbonaceous materials for silicon production. Ph.D. Thesis 30. NTNU, Trondheim, Norway, 232 pp.

Nygaard, L., 2006. Silicon solidification techniques for the chemical industry. Proceedings of the Conference on Silicon for the Chemical Industry, NTNU, Trondheim. 12–15 June 2006, 71–78.

Ringdalen, E., Tangstad, M., 2012. Reaction mechanisms in carbothermic production of silicon, study of selected reactions. Proceedings of the International Smelting Technology Symposium, Hoboken, NJ: John Wiley & Sons, 195–204.

Roskill International, 2011. Silicon and Ferrosilicon: Global Industry Markets and Outlook, thirteenth edition. 268 pp.

Schei, A., Tuset, J.K., Tveit, H., 1998. Production of High Silicon Alloys. Trondheim: Tapir Forlag, 363 pp.

Schnurre, S.M., Gröbner, J., Schmid-Fetzer, R., 2004. Thermodynamics and phase stability in the Si–O system. Journal of Non-Crystalline Solids 336, 1–25.

Shkirmontov, A.P., 2009a. Theoretical principles and energy parameters in ferrosilicon production with an increase in the electrode spacing and the distance from the electrodes to the bath. Metallurgist 53 (5–6), 373–379.

Shkirmontov, A.P., 2009b. Energy parameters of ferrosilicon production with larger-than-normal values for the electrode gap and electrode spacing under factory conditions. Metallurgist 53 (9–10), 642–647.

Swensson, A., Kvarnström, K., Bruce, T., Edling, N.P.G., Glömme, J., 1971. Pneumoconiosis in ferrosilicon workers – a follow-up study. Journal of Occupational Medicine 13 (9), 427–432.

Tang, K., Øvrelid, E.J., Tranell, G., Tangstad, M., 2010. Thermochemical and kinetic databases for the solar cell silicon materials. Proceedings of the Congress Infacon-XII, Helsinki, Finland. 2, 619–629.

Vishu, D., Kroupa, M., Bittar, R., 2005. Silicon and silicon alloys, chemical and metallurgical. In: Kirk-Othmer Encyclopedia of Chemical Technology, volume 21. John Wiley, NY, pp. 1104–1122.

Young, L.E., 2001. Ferroalloys: production and use in steelmaking. In: Encyclopedia of Materials: Science and Technology. Elsevier, pp. 3039–3044.

Zubov, V.L., Gasik, M.I., 2002. Electrometallurgy of Ferrosilicon. Dnepropetrovsk: System Technologies Publ., 704 pp.